SPONTANEOUS VORTICES IN FERROMAGNET-SUPERCONDUCTOR SYSTEMS

A Dissertation

by

HONGDUO WEI

Submitted to the Office of Graduate Studies of
Texas A&M University
in partial fulfillment of the requirements for the degree of

DOCTOR OF PHILOSOPHY

May 2006

Major Subject: Physics

SPONTANEOUS VORTICES IN FERROMAGNET-SUPERCONDUCTOR SYSTEMS

A Dissertation

by

HONGDUO WEI

Submitted to the Office of Graduate Studies of
Texas A&M University
in partial fulfillment of the requirements for the degree of

DOCTOR OF PHILOSOPHY

Approved by:

Chair of Committee,	Valery L. Pokrovsky
Committee Members,	Roland E. Allen
	Stephen Fulling
	Joseph Ross
Head of Department,	Edward Fry

May 2006

Major Subject: Physics

ABSTRACT

Spontaneous Vortices in Ferromagnet-Superconductor Systems. (May 2006)

Hongduo Wei, B.S., Zhejiang University;

M.S., Chinese Academy of Sciences;

M.S., Texas A&M University

Chair of Advisory Committee: Dr. Valery L. Pokrovsky

We study the interaction between superconductors and ferromagnets in two systems: a ferromagnet-superconductor bilayer, and a thin superconducting film with a periodic array of magnetic dots upon it, with spontaneous vortices appearing in the systems. We show that the superconducting phase transition is of the first order in a ferromagnet-superconductor bilayer and of the second order in the superconducting film with a periodic array of magnetic dots upon it. The shift of the transition temperature, ΔT_c, due to the presence of a ferromagnetic layer may be positive or negative in the ferromagnet-superconductor bilayer and is always negative in the superconducting film with a periodic array of magnetic dots upon it. The dependence of ΔT_c on geometrical factors and the external magnetic field is found. The theory is extended to multilayer structures. Next, we study the anisotropy dependence of the critical current in a thin superconducting film with a periodic array of magnetic dots with magnetization perpendicular to the film with spontaneous vortices and antivortices. The phase diagrams for the appearance of spontaneous vortices and antivortices are given for the square arrays of circular and square F dots respectively when the direction of the magnetization is parallel to the superconducting film.

To my father

ACKNOWLEDGMENTS

I would like to express my sincere appreciation to my advisor, Dr. Pokrovsky, who has helped and encouraged me to gain my Ph.D degree during the past few years. I am also thankful to all my committee members, Dr. Allen, Dr. Fulling, and Dr. Ross, for their willingness to serve on my committee. This work was supported by the NSF under the grants DMR 0321572 and DMR-0103455, by the DOE under the grant DE-FG03-96ER45598 and by Telecommunications and Informatics Task Force at Texas A&M University.

TABLE OF CONTENTS

LIST OF TABLES

LIST OF FIGURES

FIGURE Page

CHAPTER I

INTRODUCTION

Superconductivity, i.e. the complete disappearance of dc electric resistivity has been detected in many metals at sufficiently low temperatures. The modern theoretical explanation of the phenomena of superconductivity dates back to 1957, when J. Bardeen, L. Cooper, and J. Schrieffer[1] created the theory of superconductivity (the BCS theory). This theory is based on Cooper's theorem about instability of the ground state of an electron gas with arbitrarily small attraction between its particles against formation of bound states, namely, electron pairs. In most cases, the attraction between electrons due to interaction between electrons and vibrations of the crystal lattice (phonons) is stronger than their direct Coulomb repulsion. This interaction generates an excess of positive charge around an electron. Although the nature of attraction between particles may vary considerably, the Cooper pair is a common mechanism responsible for formation of superfluid states in various systems. Not all electrons do this, but only those within a Debye energy of the Fermi surface. The characteristic dimension of a Cooper pair is $\xi = \hbar v_F / 2\pi T_c$, where T_c is the transition temperature of superconductors. Cooper pairs cannot be treated as isolated composite particles, and the problem of formation of the superconducting states is essentially a many-body problem. Cooper pairs are composed of particles with spin 1/2. The spin component of a pair wave function can characterized by its total spin $S = 0$ (singlet) or $S = 1$ (triplet).

Superconductivity (with singlet Cooper pairs) and ferromagnetism are two competing phenomena: while the first prefers anti-parallel spin orientation of electrons in

---

The journal model is Physics Review B.

Cooper pairs, the second forces the spins to be aligned parallel. Their coexistence the same material or their interaction in spatially separated materials leads to a number of new interesting phenomena, for example, the π-state of superconductor-ferromagnet-superconductor Josephson junctions[2], and the non-monotonic dependence of the critical temperature T_c of superconductor-ferromagnet bilayers as a function of the ferromagnet thickness [3]. All the above mentioned are due to the proximity effect and based on the Larkin-Ovchinnikov -Fulde-Ferrel (LOFF) effect[4]. The basic idea is that when a singlet Cooper pair penetrates into a Ferromagnet, the electron with spin projection parallel to the exchange field acquires the energy $-h$, whereas the electron with anti-parallel spin acquires the energy $+h$. Their Fermi momenta therefore split by the value $q = 2h/v_F$. The Cooper pair acquires such a momentum and the order parameter oscillates. In our following discussion, however, the proximity effect is suppressed due a oxide layer between the ferromagnet and superconductor components.

Heterogeneous ferromagnet-superconductor systems without the proximity effect [5, 6, 7, 8, 9, 10, 11, 12, 13, 14, 15, 16, 17, 18, 19, 20, 21, 22, 23, 24, 25, 26, 27, 28, 29, 30, 31, 32, 33, 34] have attracted much attention recently. The ferromagnetic and superconducting components interact via magnetic fields. Any inhomogeneous magnetization produces a magnetic field penetrating into the superconductor and inducing supercurrents. The supercurrents in turn generate a magnetic field acting on the magnetization. Systems in which both, ferromagnetic and superconducting parts are thin films represent a special interest for the experimentalists and can be analyzed theoretically. In these systems, spontaneous vortices appear due to the magnetic interaction[19]. Erdin *et al.*[20] have developed a method to calculate the arrangement of the magnetization in the ferromagnetic film and supercurrents including vortices and antivortices in the superconducting film in the London's approxima-

tion. The London's approximation is justified for these mesoscopic systems because characteristic length scales for magnetic field (the effective penetration depth and the period of textures) are much larger than the coherence length ξ of the superconductor. This method was applied recently [21] to study topological textures in the ferromagnet-superconductor bilayer . It was shown that the homogeneous state of the ferromagnet-superconductor bilayer with the magnetization perpendicular to the layer is unstable with respect to the formation of vortices. The ground state of the ferromagnet-superconductor bilayer represents a periodic array of stripe domains in which the direction of the magnetization in the ferromagnetic film and the vorticity in the superconducting film alternate together.

Another interesting phenomenon is the pinning of vortices by ferromagnetic dots. Strong periodic pinning forces in these systems depend on the size of the dots, their magnetization, the distances between them, and geometry of the array. They also depend on temperature and the external magnetic field. The effective penetration depth of the superconducting-film, $\lambda_e = \lambda_L^2/d_s$, depends on temperature (λ_L is the London penetration depth and d_s is the thickness of the superconducting-film). Therefore, the interaction energy between vortices and ferromagnetic-dots, which is a function of λ_e, changes with temperature. As any other vortex lattices interacting with periodic pinning arrays, these systems display commensurability effects when the number of vortices in the superconducting-film is a multiple or rational multiple of the number of the ferromagnetic-dots [25, 26, 27, 28]. At weak magnetization the dots do not generate vortices, but pin the vortices induced by an external magnetic field. At larger values of magnetization each dot creates only one vortex pinned at the dot center. At even larger values of the magnetization (or radius) more vortices appear[20]. Since the total flux from a dot is zero, interstitial antivortices must appear. Their positions are determined by their interaction with the ferromagnetic-dots and other vortices.

The interstitial vortices, though created by an external magnetic field rather than by dots, cause the Shapiro steps observed by Van Look *et al.* [29] and described theoretically by Reichardt *et al.* [25]. For a general review, see reference [30].

In our research work, we use the static London-Maxwell equation to study the vortices and the magnetization arrangement for a system of interacting superconductors and ferromagnets separated in space. The homogeneous state of a ferromagnet-superconductor bilayer with the magnetization perpendicular to the layer becomes unstable with respect to the formation of vortices in the superconducting layer at some condition. The developing topological instability in the ferromagnet-superconductor bilayer leads to formation of stripes in which the direction of the magnetization in the magnetic film and the direction of vorticity in the superconducting film alternate together. This stripe structure has been predicted by Erdin *et al.*[21], in corrected form by Pokrovsky and Wei[32]. We study the superconducting phase transition in this system. This is a first order phase transition because in the normal phase the magnetic film itself is in stripe structure and this structure will cut the superconducting phase transition when its energy is lower than the vortices stripe structure. Then, the superconducting order parameter changes dis-continuously to zero when the temperature is raised to T_c. This means that it is a first order phase transition. We calculate the shift of the transition temperatures in the system. Because the spontaneous stripe structure will always lower the total free energy, it can be shown that the shift of the transition temperatures can be positive. This in nontrivial since the stray field of the ferromagnet usually decreases the transition temperature. Next, we study how the stripe widths change in an external magnetic field. We show that the stripe width with magnetization parallel to the external field is increased while the stripe width with magnetization anti-parallel to the external field is decreased. The critical external field to destroy the stripe structure is predicted which is about 1

to 10 Oersted. Simultaneously, the transition temperature may change by the value $\Delta T_c/T_c \sim -0.03$ to 0.02.

We then generalize these considerations to the multilayer case in the condition $Nd \ll R_s$. N is the number of superconducting layers; d is the distance between two neighboring superconducting layer.; R_s is the lateral size of the films. The $1/N$ vortex results is obtained for a N layer superconducting film. Here $1/N$ vortex means that each vortex carries a Φ_0/N flux quantum. The energy of the linear vortex and interaction energy between them is given. We also find that the critical magnetic field at which the stripe disappears increases with the number of layers N. The shift of the transition temperature can change sign from negative to positive with N increasing. The reduction of the transition temperature in the superconducting film with array of magnetic dots may be of the same order of magnitude as in the stripe structure at reasonable values of parameters. In the ferromagnet-superconductor multilayer, this magnitude is the same as that in a single isolated ferromagnet-superconductor bilayer.The stripes are expected to appear in the multilayer samples whose total thickness is much smaller than their lateral size. No stripes will exist in the opposite limiting case. This implies that there must exist a critical value of ratio of the thickness to the transverse size, at which the stripe structure disappears. The accepted approximation does not allow one to calculate this ratio and the corresponding critical behavior.

Secondly, we consider a superconducting film with array of magnetic dots structure (with magnetization perpendicular to the film). It has been shown that a spontaneous vortex -antivortex array can appear in the system[22]. We explain why the periodicity of vortex array can be broken. The reason is that the interaction between a vortex and a ferromagnetic dot is a short range one, whereas the interaction between a vortex and an antivortex is long range. If the lattice constant is large enough

compared to the effective penetration depth, the antivortices are attracted by the vortices and deviate from the center of the unit cell. This is a symmetry violation. We then find that the superconducting phase transition is of the second order and that the shift of the transition temperature ΔT_c is negative and is about 0.1 K. We next study the anisotropy and temperature dependence of the critical current in a superconducting film with array of magnetic dots with magnetization perpendicular to the film and sufficiently large to generate vortices in the superconducting film under each dot and antivortices between the ferromagnetic dots. Assuming that the vortices do not move(due to the strong pinning force by the ferromagnetic dots), we calculate the velocity of the antivortices and the induced electric field driven by the DC current exceeding its critical value. We predict the appearance of Shapiro steps in this system.

The plan of this dissertation is as follows: In chapter II, we consider the change of the transition temperatures due to spontaneous stripe structures in the ferromagnet-superconductor bilayer; we analyze how this stripe structure and the transition temperatures change in the presence of an external magnetic field; we study the shift of the transition temperatures in the superconducting film with array of magnetic dots; In the end of the chapter II, the theory of spontaneous textures in a multilayer ferromagnet-superconductor structure and the shift of the transition temperatures in it are presented.

In chapter III, we study the anisotropy and temperature dependence of the critical current in a superconducting film covered with a regular square array of ferromagnetic dots with magnetization perpendicular to the film sufficiently large to generate vortices in the superconducting film under each dot and antivortices between dots. Assuming that the vortices do not move, we calculate the velocity of the antivortices and the induced electric field driven by the dc current exceeding its critical value.

In chapter IV, we study the interaction between superconducting vortices and ferromagnetic dots with in-plane magnetization. If the size of a ferromagnetic dot is large enough, the spontaneous vortices appear easily at the boundary of the dot. For a circular ferromagnetic dot with the diameter close to the lattice constant, the number of vortices appearing is necessarily even. We argue that the system of vortices has the same symmetry as the original array of ferromagnetic dots, whereas the symmetry may be broken spontaneous if the magnetization of the dots is perpendicular to the superconducting film. We calculate the phase diagrams of different vortex phases for square arrays of circular and square dots.

In chapter V, we present the conclusions. In the Appendix, the basic method in our calculation is given.

CHAPTER II

SUPERCONDUCTING TRANSITION TEMPERATURE IN HETEROGENEOUS FERROMAGNET-SUPERCONDUCTOR SYSTEMS

In this chapter we study the superconducting transition in heterogeneous ferromagnet-superconductor systems including the ferromagnet-superconductor bilayer, multilayers and superconducting film with ferromagnetic dots. For this purpose we extend the theory of spontaneous ferromagnet-Superconductor structures developed in the work of Ref. [21] to the case of multilayers. We demonstrate that in the ferromagnet-superconductor bilayer the transition proceeds discontinuously (with a first order phase transition) as a result of competition between the stripe domain structure in a ferromagnetic layer when the superconducting layers in normal state and the combined vortex-domain structure in the ferromagnet-superconductor bilayer. Spontaneous vortex-domain structures in the ferromagnet-superconductor bilayer tend to increase the transition temperature, whereas the effect of the ferromagnetic self-interaction decreases it. The final shift of transition temperature ΔT_c depends on several parameters characterizing the superconducting and ferromagnetic films and varies typically between -$0.03T_c$ and $0.03T_c$.

In the superconducting film with ferromagnetic dots the superconductivity appears continuously (the second order phase transition). The shift of the transition temperature is always negative in this system.

Though the influence of the textures on the transition temperature is akin to the influence of the homogeneous magnetic field, there are important differences between these two phenomena: first, the average magnetic field may be zero for magnetic textures; second, the reciprocal action of the magnetic field generated by V onto magnetization is substantial.

The plan of this chapter is as follows. In the following section A we consider the change of the transition temperature due to spontaneous stripe structures in the ferromagnet-superconductor bilayer. In Sec. B we analyze how this stripe structure and the transition temperature change in the presence of an external magnetic field. In Sec. C we study the shift of the transition temperature in the superconducting film with ferromagnetic dots. Sec. D is devoted to theory of spontaneous textures in a multilayer ferromagnet-Superconductor structure and to the shift of the transition temperature in it.

A. Transition temperature in the spontaneous stripe structure of ferromagnet-superconductor bilayer

As it was shown in Ref.[21], the homogeneous state of the ferromagnet-superconductor bilayer with the magnetization perpendicular to the layer is unstable with respect to the formation of a stripe domain structure, in which both the direction of the magnetization in the ferromagnetic film and the circulation of the vortex in the superconducting film alternate together. Let the stripe width be L_s. The magnetization can be written as $\mathbf{m} = ms(x)\hat{z}$, where the coordinate x is along the direction perpendicular to the domain walls, $\hat{z}$ denotes the unit vector perpendicular to the layers, and $s(x)$ is a periodic step function with period $2L_s$:

$$s(x) = \begin{cases} +1 & 0 < x < L_s, \\ -1 & L_s < x < 2L_s. \end{cases}$$

The energy of the stripe structure per unit area U and the equilibrium stripe width L_s were calculated in [21]. Here we correct a calculation's mistake of that work[35]:

$$U = \frac{-16\tilde{m}^2}{\lambda_e} \exp\left(\frac{-\tilde{\epsilon}_{dw}}{4\tilde{m}^2} + C - 1\right), \tag{2.1}$$

$$L_s = \frac{\lambda_e}{4} \exp(\frac{\tilde{\epsilon}_{dw}}{4\tilde{m}^2} - C + 1)\,. \tag{2.2}$$

The notations in Eqs. (2.1) and (2.2) are as follows: $\lambda_e = \lambda^2/d_s$ is the effective penetration depth of the superconducting film, whose thickness is denoted d_s; λ is the London penetration depth; $\tilde{\epsilon}_{dw}$ is the renormalized linear tension of the domain wall; $\epsilon_v = \frac{\phi_0^2}{16\pi^2\lambda_{eff}} \ln \frac{\lambda_e}{\xi}$ is the single vortex energy in the absence of the ferromagnetic film; m is the magnetization per unit area of the ferromagnetic film; $\tilde{m} = m - \epsilon_v/\phi_0$ is the renormalized magnetization (due to the screening effect of vortex); $C \approx 0.57721$ is the Euler constant. To find the transition temperature, we combine the energy given by Eq. (2.1) with the Ginzburg-Landau free energy. The total free energy per unit area reads:

$$\begin{aligned} F = U + F_{GL} = \frac{-16\tilde{m}^2}{\lambda_{eff}} \exp(\frac{-\tilde{\epsilon}_{dw}}{4\tilde{m}^2} + C - 1) \\ + n_s d_s[\alpha(T - T_c) + \frac{\beta}{2} n_s]\,. \end{aligned} \tag{2.3}$$

Here α and β are the Ginzburg-Landau parameters. We have omitted the gradient term in the Ginzburg-Landau equation since the gradient of the phase is included in the energy (2.1), whereas the gradient of the superconducting electron density can be neglected everywhere beyond the vortex cores. Recalling that $\lambda^2 = \frac{m_s c^2}{4\pi n_s e^2}$ and plugging it into Eq. (2.3), we find the free energy as function of n_s, $T - T_c$ and m. Note that

$$\tilde{m} = m + \frac{\phi_0 e^2 d_s n_s}{4\pi m_s c^2} \ln \frac{4\pi e^2 d_s n_s \xi}{m_s c^2}\,. \tag{2.4}$$

We expect that n_s is small near the transition point T_c and, therefore, retain only the linear in n_s part in the first term in Eq. (2.3). This term can be included in the Ginzburg-Landau free energy and resulting in a shift of the Ginzburg-Landau

transition temperature:

$$F = n_s d_s[\alpha(T - T_r) + \frac{\beta}{2} n_s]\,, \tag{2.5}$$

where

$$T_r = T_c + \frac{64\pi m^2 e^2}{\alpha m_s c^2} \exp(\frac{-\tilde{\epsilon}_{dw}}{4m^2} + C - 1)\,. \tag{2.6}$$

Minimizing the total free energy over n_s, we find the equilibrium value of n_s (for $T < T^r$): $n_s = -\frac{\alpha}{\beta}(T - T_r)$. Substituting it back to Eq. (2.5), we find the equilibrium free energy:

$$F = -\frac{\alpha^2 (T - T_r)^2}{2\beta} d_s\,. \tag{2.7}$$

The superconducting phase is stable if its free energy (2.7) is less than the free energy of a single ferromagnetic film with the stripe domain structure, which has the following form[36, 37]: $F_{fm} = -\frac{4m^2}{L_f}$, where L_f is the stripe width of the single ferromagnetic film. Near the superconducting transition point the temperature dependence of the variation of this magnetic energy is negligible. Hence, when T increases, the superconducting film transforms into a normal state at some temperature T_c^* below T_r. This is a first order phase transition. At the transition point both energies equal to each other:

$$\frac{\alpha^2 (T_c^* - T_r)^2}{2\beta} d_s = \frac{4m^2}{L_f}\,. \tag{2.8}$$

Thus, the shift of the transition temperature is determined by a following equation:

$$T_c^* - T_c = \frac{64\pi m^2 e^2}{\alpha m_s c^2} \exp(\frac{-\tilde{\epsilon}_{dw}}{4m^2} + C - 1) - \sqrt{\frac{8\beta m^2}{\alpha^2 d_s L_f}}\,. \tag{2.9}$$

Two terms in Eq. (2.9) play opposite roles. The first one is due to the appearance of spontaneous vortex which lowers the free energy of the system and tends to increase the transition temperature. The second term is the contribution of the purely magnetic energy, which tends to decrease the transition temperature. The values

of parameters entering equation (2.9) can be estimated as follows. The dimensionless Ginzburg-Landau parameter is $\alpha = 7.04T_c/\epsilon_F$, where ϵ_F is the Fermi energy. A typical value of α is about 10^{-3} for low-temperature superconductors. The second Ginzburg-Landau parameter is $\beta = \alpha T_c/n_e$, where n_e is the electron density. For estimates we take $T_c \sim 3K$, $n_e \sim 10^{23}$ /cm^3. The magnetization per unit area m is the product of the magnetization per unit volume M and the thickness of the ferromagnetic film d_m. We accept a typical value of $M \sim 10^2$ Oe, and $d_m \sim 10^2$ Å. Then $m = 10^{-4}$ Gs/cm^2. In an ultra-thin magnetic film the observed values of L_f vary in the range 1 to 100 μm[38, 39]. If $L_f \sim 1$ μm, $d_s = d_m = 10^2$ Å, and $\exp(-\tilde{\epsilon}_{dw}/4m^2 + C - 1) \approx 10^{-3}$, we obtain $\Delta T_c/T_c \sim -0.03$. For $L_f = 100$ μm, $d_s = 5 \times 10^2$ Å, and $\exp(-\tilde{\epsilon}_{dw}/4m^2 + C - 1) \approx 10^{-2}$, we find that $\Delta T_c/T_c \sim 0.02$.

B. Spontaneous stripe structure in an external magnetic field

In this section we study the spontaneous stripe system in the ferromagnet-Superconductor bilayer in the presence of an external perpendicular magnetic field $\mathbf{B}$ (along the $\hat{z}$ direction). Since the external magnetic field tends to align the magnetization parallel to itself, we anticipate that the width L_1 of stripes with the magnetization parallel to the external magnetic field increases, whereas the width L_2 of the stripes with the antiparallel magnetization decreases. Let us define a step function with the period $L = L_1 + L_2$ as follows:

$$s(x) = \begin{cases} +1 & (0 < x < L_1), \\ -1 & (L_1 < x < L). \end{cases}$$

The Fourier-transform of $s(x)$ is:

$$s_G = \begin{cases} 2i(1-e^{iGL_1})/(LG) & (G \neq 0), \\ (L_1 - L_2)/L & (G = 0). \end{cases} \tag{2.10}$$

Here $G = 2\pi r/L$ and $r = 0, \pm 1, \pm 2, \cdots$. For the sake of brevity, we denote $t = L_1 - L_2$. At large distance from the bilayer the magnetic field asymptotically becomes equal to the external magnetic field. The total magnetic flux is the same in any cross-section of the space. Thus, the average magnetic field through the superconducting layer is

$$\frac{\phi_0}{L}\int_0^L n(x)dx = B_{ext}\,, \tag{2.11}$$

where $n(x)$ is the density of vortex. The general expression for the free energy of a periodic stripe system of magnetization and vortex is given by Eq. (10) of the work [21]. Employing this equation and the Fourier expansion for the step function $s(x)$ (see Eq. (2.10)) and denoting n_G the Fourier-transform of the vortex density $n(x)$, we obtain:

$$U_v = \sum_G \tilde{\epsilon}_v s_G n_{-G} + \frac{1}{2}\sum_{G\neq 0} V_G n_G n_{-G}\,, \tag{2.12}$$

where $\tilde{\epsilon}_v = \epsilon_0 - m\phi_0$ is the renormalized energy of a vortex. $V_G = \phi_0^2/(2\pi|G|)$ is the Fourier-transform of the vortex interaction energy. An infinitely large term $V_{G=0}n_{G=0}^2$ has been omitted since it corresponds to the energy of the external magnetic field. From Eq. (2.12) we readily find that the constraint condition implies:

$$n_{G=0} = \frac{B_{ext}}{\phi_0}\,. \tag{2.13}$$

This equation confirms that $V_{G=0}n_{G=0}^2$ is the energy of the uniform external field. Minimization of the total vortex energy U_v over the vortex density $n_{\mathbf{G}}$ results in equations:

$$\tilde{\epsilon}_v s_G + V_G n_G = 0 \quad (G \neq 0)\,. \tag{2.14}$$

Plugging the solutions n_G from Eqs. (2.13) and (2.14) into Eq. (2.12) and adding the energy of domain walls, we arrive at the following expression for the total energy per unit area:

$$\begin{aligned}\tilde{U} &= \frac{-8\tilde{m}^2}{L}[C + \ln\frac{L}{\lambda_e} + \frac{1}{2}\ln(2 + 2\cos\frac{\pi t}{L})] \\ &\quad -\frac{\tilde{m}B_{ext}t}{L} + \frac{2\epsilon_{dw}}{L}\,. \end{aligned} \tag{2.15}$$

Minimizing the total energy U over L and t, we find the equilibrium values of L and t:

$$L = \frac{2L_s}{\sqrt{1 - (\frac{L_s B_{ext}}{2\pi\tilde{m}})^2}}\,, \tag{2.16}$$

$$t = \frac{2L}{\pi}\arctan\frac{LB_{ext}}{4\pi\tilde{m}}\,. \tag{2.17}$$

where L_s is given by Eq. (2.2). The results of Eqs. (2.16) and (2.17) are similar to those for a purely ferromagnetic stripe structure in a single ferromagnetic film[40]. The critical external field B^c_{ext} at which the domain structure vanishes is

$$B^c_{ext} = 2\pi\tilde{m}/L_s\,. \tag{2.18}$$

It varies in the range of $1 \div 10$ Oe.

In the end of this section, we consider how the superconducting transition temperature of the bilayer changes in the presence of external magnetic field. Since at a field $B^c_{ext} \sim 1 \div 10$ Oe the stripe structure vanishes, the superconducting transition proceeds in the homogeneous state of ferromagnetic film excluding very small vicinity of T_c. Therefore, it is determined by the same nucleation process as in the case of a single superconducting film. The nucleation in a thin film for the field perpendicular to it was considered by Tinkham [41]. Though the geometry is different from the bulk geometry considered by Abrikosov [42], his solution can be applied directly. The

order parameter coincides with the Landau wave function for the first Landau level. In the case of the bilayer the energy of the nucleus reads:

$$U = \int \left[\frac{1}{2m} \left| \left(\frac{\hbar}{i} \nabla - \frac{2e}{c} \mathbf{A}_0 \right) \psi \right|^2 + a \left| \psi \right|^2 \right] d^2x + \Delta U \, . \tag{2.19}$$

Here $\mathbf{A}_0$ is the vector potential produced by the critical field $\mathbf{H}_{c2}$. The nucleus energy (2.19) differs from that in the absence of magnetic film by the value $\Delta U = -m \int B_z^{(n)} d^2x$, where $B_z^{(n)}$ is the magnetic field generated by the nucleus at the ferromagnetic film. We will prove that this additional term is equal to zero. Indeed, the magnetic field generated by the nucleus reads:

$$\mathbf{B}^{(n)}(\mathbf{x}) = \frac{1}{c} \int \nabla \frac{1}{|\mathbf{x} - \mathbf{x}'|} \times \mathbf{j}_n(\mathbf{x}') d^3x' \, , \tag{2.20}$$

where $\mathbf{x}'$ is a point inside superconducting film, whose thickness will be put zero in the end; $\mathbf{x}$ denotes a point in the ferromagnetic film. We assume that the current flows in the $x - y$ plane. Since it has zero divergence, it can be represented as $\mathbf{j}_n = \hat{z} \times \nabla' f(x', y')$, where $f(x', y')$ is a function localized in a finite part of the superconducting film. The flux of the induced field is:

$$\int B_z^{(n)} d^2x = \\ \frac{1}{c} \int \left(\hat{z} \times \nabla \frac{1}{|\mathbf{x} - \mathbf{x}'|} \right) \left(\hat{z} \times \nabla' f(\mathbf{x}') \right) d^2x d^3x' \, . \tag{2.21}$$

A simple transformation turns this integral into a following form:

$$\int B_z^{(n)} d^2x = \frac{1}{c} \int f(\mathbf{x}') \nabla^2 \frac{1}{|\mathbf{x} - \mathbf{x}'|} d^2x d^3x' \, . \tag{2.22}$$

This integral is equal to zero if $\mathbf{x}$ and $\mathbf{x}'$ belong to different films. Thus, the interaction between the superconducting nucleus and the homogeneously magnetized film is zero independent of the wave function of the localized nucleus. Therefore, the transition

temperature is the same as that in the absence of the ferromagnetic film.

Let the external magnetic field B_{ext} equal to the value, at which the stripe structure in a single ferromagnetic film vanishes $B_c = 2\pi m/L_f$ [40]. In the interval of magnetic field $B_c < B < H_{c2}$ the shift of the transition temperature is the same as in the absence of the ferromagnetic layer $\Delta T_c/T_c = B/H_{c2}$. The typical value of B_c is $\sim 1 \div 10$ Oe. On the other hand, the second critical field for the superconducting film at $T = T_c^*$ can be estimated as $H_{c2}(T_c^*) = H_{c2}(T = 0)|T_c - T_c^*|/T_c \sim 100$ Oe. Hence $B_c < H_{c2}(T_c^*)$. It confirms our assumption that the ferromagnetic film remains homogeneous at the superconducting transition. From the formulae $T_c^* = T_c(1 - B_{ext}/H_{c2})$ and $B_c = 2\pi m/L_f$ we find the shift of the transition temperature due to B_c is $|\Delta T_c|/T_c = B_c/H_{c2}(0) \sim 10^{-3} \div 10^{-2}$. For large L_f the sensitivity of the shift of the transition temperature to the magnetic field can be rather strong.

C. Transition temperature in a superconducting film with a square array of ferromagnetic dots

Recently Erdin considered theoretically the vortex-antivortex textures in superconducting film with ferromagnetic dots[22]. For the case that only one vortex and one antivortex appear per a magnetic dot, he predicted a symmetry violation in the lowest energy state in a range of parameters. For simplicity we choose another range of parameters in which no symmetry violation occurs: the vortex centers are located precisely under the centers of the magnetic dots, whereas the antivortex centers are located between them in the centers of elementary cells. Let us assume each dot to be a circular thin disk with a radius R and a constant magnetization m per unit area with a direction perpendicular to the plane (along the z-axis). Let a denote the dot lattice constant. Fig. 1 schematically represents ferromagnetic dots with spontaneous

vortex and antivortex. The circles drawn by solid line represent ferromagnetic dots. The dashes half-circles with clockwise and counterclockwise arrow indicate vortex and antivotex respectively. The total energy per unit area of the system is[22]:

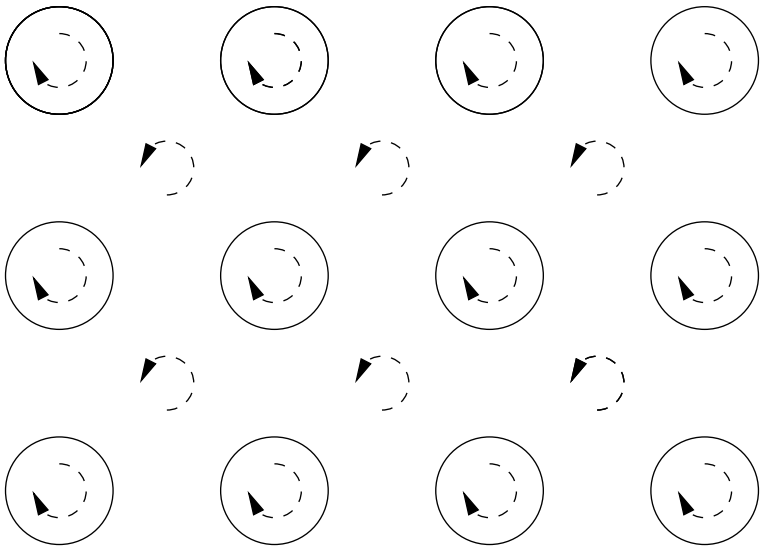

Fig. 1. Schematics representation of ferromagnetic dots with spontaneous vortex and antivortex. The circles drawn by solid line represent ferromagnetic dots. The dashes half-circles with clockwise and counterclockwise arrow indicate vortex and antivotex respectively.

$$U = u_{vv} + u_{mv} + u_{mm}\,. \tag{2.23}$$

The three terms in the right-hand side of the above equation have the following forms:

$$u_{vv} = \frac{\phi_0^2}{4\pi a^4}\sum_{\mathbf{G}}\frac{|F_{\mathbf{G}}|^2}{G(1+2\lambda_e G)}\,, \tag{2.24}$$

$$u_{mv} = -\frac{\phi_0}{a^2}\sum_{\mathbf{G}}\frac{m_{z\mathbf{G}}F_{-\mathbf{G}}}{1+2\lambda_e G}\,, \tag{2.25}$$

$$u_{mm} = -2\pi\lambda_e\sum_{\mathbf{G}}\frac{G^2|\mathbf{m}_{z\mathbf{G}}|^2}{1+2\lambda_e G}\,. \tag{2.26}$$

where $\mathbf{G} = \frac{2\pi}{a}(r,s)$ (r, s are integers) are the reciprocal lattice vectors; $F_{\mathbf{G}} = \sum_i n_i e^{i\mathbf{G}\cdot\mathbf{r}_i}$ is the structure factor of the vortex lattice; n_i and $\mathbf{r}_i$ indicate the vorticity and the position of the i-th vortex in the elementary cell, respectively. In the purely magnetic term, u_{mm}, it is necessary to perform a regularization (here regularization means that the ground energy of the magnetic film is shifted by a constant which is independent of the superconductor as will be shown by Eq. (2.27)) since only the difference between energies of the superconducting and normal state matters:

$$u_{mm} \to \tilde{u}_{mm} = u_{mm}(\lambda_e) - u_{mm}(\lambda_e = \infty)\,. \tag{2.27}$$

The last term in the r.-h.s. of Eq. (2.27) is the dipolar energy of the ferromagnetic dots above the superconducting transition. At temperature below the superconducting transition the magnetic field generated by the dots penetrates into the superconducting film and creates vortex and antivortex if the magnetization and the size of the dots are large enough [20]. Keeping in mind that $\lambda_e \gg a$ near the new transition temperature T_c^*, we can rewrite the total energy Eq. (2.23) as follows:

$$\begin{aligned} u &= \frac{\phi_0^2 e^2 d_s n_s}{2\pi m_s c^2 a^2}\ln\frac{a}{\xi} - \frac{\phi_0^2 e^4 d_s^2 n_s^2}{4\pi^2 m_s^2 c^4 a} I_0 \\ &\quad - \frac{\phi_0^2 e^2 d_s n_s}{4\pi^2 m_s c^2 a^2}(I_1 + \frac{4\pi^2 mR}{\phi_0} I_2) \\ &\quad + \frac{2\pi^2 m^2 e^2 d_s n_s R^2}{m_s c^2 a^2} I_3\,. \end{aligned} \tag{2.28}$$

where $\sum'$ means that the term $r = s = 0$ is omitted. I_1, I_2 and I_3 are defined as series:

$$\begin{aligned} I_0 &= \sum_{n,s=-\infty}^{+\infty\,\prime} \frac{1}{(n^2+s^2)^{3/2}}\,, \\ I_1 &= \sum_{n,s=-\infty}^{+\infty\,\prime} \frac{(-1)^n + (-1)^s}{n^2+s^2}\,, \end{aligned}$$

$$
\begin{aligned}
I_2 &= \sum_{n,s=-\infty}^{+\infty\,\prime} \frac{J_1(\frac{2\pi R}{a}\sqrt{n^2+s^2})[1-(-1)^{n+s}]}{n^2+s^2}\,, \\
I_3 &= \sum_{n,s=-\infty}^{+\infty\,\prime} \frac{J_1^2(\frac{2\pi R}{a}\sqrt{n^2+s^2})}{n^2+s^2}\,.
\end{aligned} \tag{2.29}
$$

We combine this energy with the Ginzburg-Landau free energy for the superconducting film as it was done in Sec. II:

$$
\begin{aligned}
F &= \frac{\phi_0^2 e^2 d_s n_s}{2\pi m_s c^2 a^2}\ln\frac{a}{\xi} - \frac{\phi_0^2 e^4 d_s^2 n_s^2}{4\pi^2 m_s^2 c^4 a} I_0 \\
&\quad - \frac{\phi_0^2 e^2 d_s n_s}{4\pi^2 a^2 m_s c^2}(I_1 + \frac{4\pi^2 mR}{\phi_0} I_2) \\
&\quad + \frac{2\pi^2 m^2 e^2 d_s n_s R^2}{m_s c^2 a^2} I_3 + [\alpha(T-T_c) + \frac{\beta}{2} n_s] n_s d_s\,.
\end{aligned} \tag{2.30}
$$

The condition of minimum over n_s from the free energy Eq. (2.30) reads:

$$
\begin{aligned}
&\frac{\phi_0^2 e^2 d_s}{2\pi m_s c^2 a^2}\ln\frac{a}{\xi} - \frac{\phi_0^2 e^4 d_s^2 n_s}{2\pi^2 m_s^2 c^4 a} I_0 \\
&- \frac{\phi_0^2 e^2 d_s}{4\pi^2 a^2 m_s c^2}(I_1 + \frac{4\pi^2 mR}{\phi_0} I_2) + \frac{2\pi^2 m^2 e^2 d_s R^2}{m_s c^2 a^2} I_3 \\
&+ \alpha(T-T_c) d_s + \beta n_s d_s = 0\,.
\end{aligned} \tag{2.31}
$$

At a new critical temperature, T_c^*, the density of superconducting carriers must be zero. Plugging $n_s(T_c^*) = 0$ into Eq. (2.31), we obtain the shift of the critical temperature:

$$
\begin{aligned}
\Delta T_c &= \frac{\hbar^2}{4\alpha m_s a^2}(\frac{4\pi^2 mR}{\phi_0} I_2 + I_1 \\
&\quad - 2\pi \ln\frac{a}{\xi} - \frac{8\pi^4 m^2 R^2}{\phi_0^2} I_3)\,.
\end{aligned} \tag{2.32}
$$

Fig. 2 shows the relation between ΔT_c and R for $\xi = 0.21a$. To ensure spontaneous occurrence of vortices the inequality $u_{mv} + u_{vv} < 0$ must be satisfied. It is equivalent

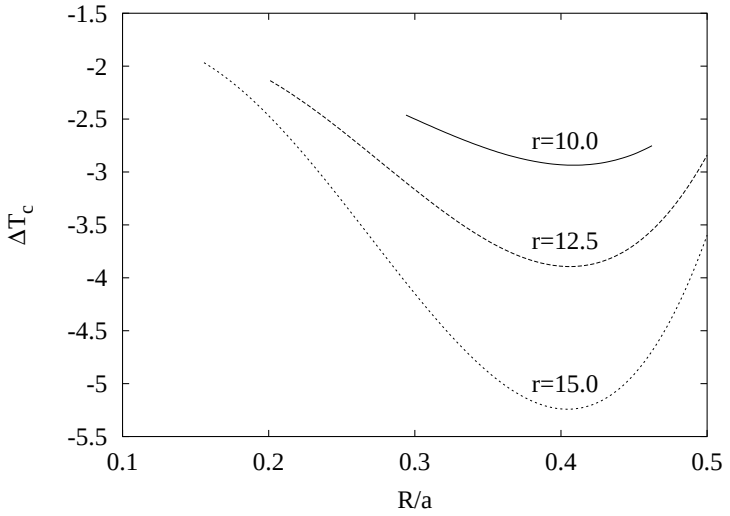

Fig. 2. The shift of the superconducting transition temperature ΔT_c vs. the dot radius R when the superconducting coherence length $\xi = 0.21a$ and $r = 10.0,\ 12,5$ and 15.0 respectively. Here $r = \frac{4\pi^2 ma}{\Phi_0}$. ΔT_c is in the unit $\frac{\hbar^2}{4\alpha m_s a^2}$, which is about 0.02 K for the Ginzburg-Landau parameter $\alpha = 10^3$ and the lattice constant $a = 3\mu$m.

to a following relation:

$$\frac{4\pi^2 mR}{\phi_0} I_2 + I_1 - 2\pi \ln \frac{a}{\xi} < 0\,. \tag{2.33}$$

The London's approximation is valid if $\xi \ll a$. This condition is violated in close vicinity of the transition temperature. For $a \sim 3\mu$m and $\xi(T = 0) = 0.1\mu$m this vicinity is of the order of $0.001T_c$ and we neglect it from now on. Fig. 2 shows that the shift of the transition temperature is a rather complicated function of the dot radius R and the ratio $r = 4\pi^2 ma/\phi_0$. For each value r, there exists a threshold radius R_0, at which the vortex first appear. The shift of the transition temperature grows by absolute value with R increasing, reaches a maximum at $R/a \approx 0.4$ and then decreases. It remains negative at any R in the interval between R_0 and $a/2$. At a fixed $R > R_0$ the absolute value of ΔT_c increases with the ratio r and is negative.

D. Ferromagnetic textures in the multilayers

We consider a ferromagnet-Superconductor multilayer system consisting of N bilayers with a distance d between two neighboring ones. Let us start with the limit $Nd \gg R_s$, where R_s is the lateral linear size of a layer. If the magnetic films are magnetized perpendicularly to the layers, the average induction inside the multilayer is $B = 4\pi m/d$ and its direction is perpendicular to the layers. The situation is the same as in a layered superconductor placed into an external magnetic field [43]. Therefore, a pancake vortex in each superconducting layer may appear (A vortex in one layer of mulitilayer superconductor is called a pancake vortex[43]). Together they form the Abrikosov linear vortex if a condition $m\phi_0/d > \epsilon_a$ is satisfied, which guarantees that the vortex line is energy favorable. Here $\epsilon_a = \epsilon_0 \ln \frac{\lambda}{\xi}$ is the vortex line energy per unit length [44], and $\epsilon_0 = \phi_0^2/(4\pi\lambda)^2$. There is no need to consider the Josephson coupling effect in this case since the phase difference between superconducting layers is zero if the vortex lines are perpendicular to the layers. On the other hand, the Josephson vortex appear along the layers if the magnetization $\mathbf{m}$ is parallel to the layers and satisfy a condition $m\phi_0/d > \epsilon_J$, where $\epsilon_J = \gamma\epsilon_0 \ln \frac{\lambda}{d}$ is the Josephson vortex line energy and γ is the anisotropy parameter for the layered superconductor [43]. These ideas were applied by M. Houzet *et al.* [45] to explain properties of the magnetic superconductor $RuSr_2GdCu_2O_8$. We will focus on a ferromagnet-Superconductor multilayer in the opposite limit $Nd \ll \Lambda \ll R_s$, where $\Lambda = \lambda^2/d$ is the effective penetration depth for layered superconductors. In such a multilayer one should expect spontaneous vortex and antivortex combined with the domains in the ferromagnetic films for the same reason as in the case of a single ferromagnet-Superconductor bilayer[21].

We first analyze a multilayer superconductor without any ferromagnetic texture. Pancake vortex in a finite stack of layers were discussed by Mints *et al.*[46]. We repro-

duce here some of their results and derive new ones by applying a modified approach proposed by Efetov [47] (see also [48]) (they considered a layered superconductor with an infinite number of layers). To simplify the calculation, we assume that layers are infinitely thin and located at the planes $z_n = nd$ (n is an integer). The vector potential $\mathbf{A_v}$ due to the pancake vortex at superconducting layers satisfies a following equation:

$$\begin{aligned} & -\Delta \mathbf{A}_v(\boldsymbol{\rho}, z) + \frac{1}{\Lambda} \sum_n \delta(z - z_n) \mathbf{A}_v(\boldsymbol{\rho}, z) \\ = \quad & \frac{\phi_0}{2\pi\Lambda} \sum_n \delta(z - z_n) \sum_{n_p} \delta_{n_p} \nabla^{(2)} \varphi_n(\boldsymbol{\rho} - \boldsymbol{\rho}_{n_p}) \,. \end{aligned} \tag{2.34}$$

The vector potential in Eq. (2.34) is induced by pancake vortex with the vorticity $\delta_{np} = \pm 1$ placed at the position $\boldsymbol{\rho}_{np}$, where p enumerates vortex in the n-th plane. The Coulomb gauge $\nabla \cdot \mathbf{A}_v = 0$ is used. In addition, $A_{vz} = 0$ because the direction of $\nabla^{(2)}\varphi_n$ is along the layers. It is useful to introduce an auxiliary potential $\tilde{\mathbf{A}}_v(\boldsymbol{\rho}, z) = \sum_n \delta(z - z_n) \mathbf{A}_v(\boldsymbol{\rho}, z)$ confined to the layers, the "London vector" [48] $\boldsymbol{\phi}_n(\boldsymbol{\rho}) = \sum_{n,p} \delta_{np} \frac{\phi_0}{2\pi} \nabla^{(2)} \varphi_n(\boldsymbol{\rho} - \boldsymbol{\rho}_{np})$, and the corresponding auxiliary vector $\tilde{\boldsymbol{\phi}}_n(\boldsymbol{\rho}, z) = \sum_n \boldsymbol{\phi}_n(\boldsymbol{\rho}) \delta(z - z_n)$. In terms of these variables Eq. (2.34) can be rewritten as follows:

$$-\Delta \mathbf{A}_v(\boldsymbol{\rho}, z) + \frac{1}{\Lambda} \tilde{\mathbf{A}}_v(\boldsymbol{\rho}, z) = \frac{1}{\Lambda} \tilde{\boldsymbol{\phi}}_n(\boldsymbol{\rho}, z) \,. \tag{2.35}$$

Eq. (2.35) can be solved by the Fourier-transformation. An intermediate result following directly from equation (2.35) reads:

$$\mathbf{A}_v(\mathbf{q}, k) = \sum_n e^{-ikz_n} \frac{\boldsymbol{\phi}_n(\mathbf{q}) - \mathbf{A}_{vn}(\mathbf{q})}{\Lambda(q^2 + k^2)} \,. \tag{2.36}$$

where $\mathbf{A}_v(\mathbf{q}, k)$ is the Fourier-transform of the vector-potential $\mathbf{A}_v(\boldsymbol{\rho}, z)$, $\mathbf{A}_{vn}(\mathbf{q})$ is the plane Fourier-transform of the vector-potential $\mathbf{A}_v(\boldsymbol{\rho}, z_n)$ taken at the $n-$th superconducting plane, and $\boldsymbol{\phi}_n(\mathbf{q})$ is the Fourier-transform of the London vector $\boldsymbol{\phi}_n(\boldsymbol{\rho})$.

Performing the inverse Fourier-transform with respect to the variable k in both sides of Eq. (2.36), we find a system of equations for $\mathbf{A}_{vn}(\mathbf{q})$ at a fixed value of $\mathbf{q}$ for each m:

$$\begin{aligned} & \sum_n (\frac{1}{2\Lambda q} e^{-q|m-n|d} + \delta_{mn}) \mathbf{A}_{vn}(\mathbf{q}) \\ = \quad & \frac{1}{2\Lambda q} \sum_n \boldsymbol{\phi}_n(\mathbf{q}) e^{-q|m-n|d} \,. \end{aligned} \tag{2.37}$$

We apply Eq. (2.37) to study the simplest case: two superconducting layers. Let only one pancake vortex be placed in the center of the layer $z = 0$ at $\boldsymbol{\rho}_1 = 0$. The other layer is located at $z = d$ without vortex on it. The solution of Eq. (2.37) for this situation reads:

$$\begin{aligned} \mathbf{A}_{v1}(\mathbf{q}) &= \frac{1 + 2\Lambda q - e^{-2qd}}{1 + 4\Lambda q + 4\Lambda^2 q^2 - e^{-2qd}} \boldsymbol{\phi}_1(\mathbf{q}) \,, \\ \mathbf{A}_{v2}(\mathbf{q}) &= \frac{2\Lambda q e^{-2qd}}{1 + 4\Lambda q + 4\Lambda^2 q^2 - e^{-2qd}} \boldsymbol{\phi}_1(\mathbf{q}) \,. \end{aligned} \tag{2.38}$$

Here $\boldsymbol{\phi}_1(\mathbf{q}) = \frac{i\phi_0}{q}\hat{\varphi}$ and $\hat{\varphi} = \hat{z} \times \hat{q}$. In the limit $qd \ll 1$ the above solution becomes simple:

$$\mathbf{A}_{v1}(\mathbf{q}) = \mathbf{A}_{v2}(\mathbf{q}) = \frac{1}{2 + 2\Lambda q} \boldsymbol{\phi}_1(\mathbf{q}) \,. \tag{2.39}$$

The current density in each layer is given by:

$$\begin{aligned} \mathbf{J}_1(\mathbf{q}) &= \frac{c}{4\pi\Lambda} (\boldsymbol{\phi}_1(\mathbf{q}) - \mathbf{A}_{v1}(\mathbf{q})) \,, \\ \mathbf{J}_2(\mathbf{q}) &= -\frac{c}{4\pi\Lambda} \mathbf{A}_{v2}(\mathbf{q}) \,. \end{aligned} \tag{2.40}$$

The asymptotic formulas for the current density in the coordinate representation are shown in the table I. The force acting between two pancake vortex is $\mathbf{F} = -\frac{\phi_0}{c}\hat{z} \times \mathbf{J}$, where $\mathbf{J}$ is the current produced by one of them at the center of another one. Table I demonstrates that the interaction energy between two pancakes with the same

Table I. The asymptotic form of the current density in each layer.

	$\rho \gg \Lambda$	$d \ll \rho \ll \Lambda$
$\mathbf{J}_1(\rho)$	$\frac{\phi_0 c}{16\pi^2 \Lambda \rho}\hat{\varphi}$	$\frac{\phi_0 c}{8\pi^2 \Lambda \rho}\hat{\varphi}$
$\mathbf{J}_2(\rho)$	$-\frac{\phi_0 c}{16\pi^2 \Lambda \rho}\hat{\varphi}$	$-\frac{\phi_0 c}{4\Lambda^2}\hat{\varphi}$

vorticity at the same layer is logarithmic and repulsive at large distance $R \gg \Lambda$ and at small distance $d \ll R \ll \Lambda$, but with different coefficients in front of the logarithm. A peculiarity of the two-layer structure is that the interaction energy of two pancake vortex with the same vorticity located in different layers and separated by the lateral distance $R \gg \Lambda$, is logarithmic but attractive. It has the same absolute value as the repulsion of two pancake vortex in the same layer. It can be interpreted as the attraction of two "half-vortices" in the two plane, one carrying the flux $+\phi_0/2$, the other carrying the flux $-\phi_0/2$. This interaction dramatically differs from the interaction of two vortex in different layers for an infinite number of layers. In the latter case the interaction in different layers is weaker than the interaction in the same layer by a small pre-factor d/λ. It can be shown that the logarithmic attraction of two pancakes in different layers with distance $R \gg \Lambda$ persists at any number of layers N provided $Nd \ll \Lambda$.

In the two-layer system the asymptotic for the components of the magnetic field produced by a pancake vortex located in the plane $z = 0$ at its origin directly follow from Eq. (2.38). In the range $\rho \gg \Lambda$ they are:

$$\begin{aligned} B_z(\rho, z) &= \frac{\phi_0}{8\pi\Lambda}\left[\frac{1}{\sqrt{\rho^2+z^2}} - \frac{1}{\sqrt{\rho^2+(z-d)^2}}\right] \\ &+ \frac{\phi_0}{8\pi}\left[\frac{|z|}{(z^2+\rho^2)^{\frac{3}{2}}} + \frac{|z-d|}{((z-d)^2+\rho^2)^{\frac{3}{2}}}\right], \end{aligned}$$

$$
\begin{aligned}
B_\rho(\rho,z) &= \frac{\phi_0}{8\pi\Lambda\rho}\mathrm{sgn}(z)(1-\frac{|z|}{\sqrt{\rho^2+z^2}}) \\
&- \frac{\phi_0}{8\pi\Lambda\rho}\mathrm{sgn}(z-d)(1-\frac{|z-d|}{\sqrt{\rho^2+(z-d)^2}}) \\
&+ \frac{\phi_0}{8\pi}\left[\frac{z}{(\rho^2+z^2)^{\frac{3}{2}}}+\frac{z-d}{(\rho^2+(z-d)^2)^{\frac{3}{2}}}\right].
\end{aligned}
$$

In another region $d \ll \rho \ll \Lambda$ we find:

$$
\begin{aligned}
B_z(\rho,z) &= \frac{\phi_0}{4\pi\Lambda\sqrt{\rho^2+z^2}}, \\
B_\rho(\rho,z) &= \frac{\phi_0}{4\pi\Lambda\rho}\mathrm{sgn}(z)(1-\frac{|z|}{\sqrt{\rho^2+z^2}}).
\end{aligned}
$$

Due to the strong screening effect exerted by one layer onto another, the magnetic field decays more quickly in the z-direction than in-plane (the ρ-direction). The total magnetic flux through the plane $z=0$ and $z=d$ are $\Phi(z=0)=B_z(\mathbf{q}=0,z=0)=\frac{\Lambda+d}{2\Lambda+d}\phi_0\approx\phi_0/2$, and $\Phi(z=d)=B_z(\mathbf{q}=0,z=d)=\frac{\Lambda}{2\Lambda+d}\phi_0\approx\phi_0/2$ respectively. The two fluxes are not exactly equal, and the net flux $\phi_0 d/(2\Lambda+d)$ escapes through the remote side surface.

The self-energy of a single pancake vortex reads:

$$
\begin{aligned}
E_{sv} &= \frac{1}{8\pi\Lambda}\int\frac{d^2q}{(2\pi)^2}[|\boldsymbol{\phi}_1(\mathbf{q})|^2-\boldsymbol{\phi}_1(-\mathbf{q})\cdot\mathbf{A}_{v1}(\mathbf{q})] \\
&= \frac{1}{8\pi\Lambda}\int\frac{d^2q}{(2\pi)^2}[\frac{\phi_0^2}{q^2}-\frac{\phi_0^2}{2q^2(1+\Lambda q)}] \\
&= \frac{\phi_0^2}{32\pi^2\Lambda}\ln\frac{R_s\Lambda}{\xi^2}. \qquad (2.41)
\end{aligned}
$$

where R_s is the lateral linear size of the layers as mentioned before. We see that E_{sv} diverges logarithmically when R_s goes to infinity. Thus, it is energy unfavorable to produce a single pancake vortex in a layer below the Berezinsky-Kosterlitz-Touless transition. The energy of a pair of pancake vortex located one opposite the other at

different planes is:

$$\begin{aligned} E_{lv} &= \frac{2}{8\pi\Lambda}\int \frac{d^2q}{(2\pi)^2}[|\boldsymbol{\phi}_1(\mathbf{q})|^2 - \boldsymbol{\phi}_1(-\mathbf{q}) \\ &\quad \cdot(\mathbf{A}_{v1}(\mathbf{q}) + \mathbf{A}_{v2}(\mathbf{q})] \\ &= \frac{1}{4\pi\Lambda}\int \frac{d^2q}{(2\pi)^2}[\frac{\phi_0^2}{q^2} - \frac{\phi_0^2}{q^2(1+\Lambda q)}] \\ &= \frac{\phi_0^2}{8\pi^2\Lambda}\ln\frac{\Lambda}{\xi}\,. \end{aligned} \tag{2.42}$$

The interaction energy of two such pairs separated by a distance $R \gg d$ is:

$$\begin{aligned} V_{ll}(R) &= \frac{2}{8\pi\Lambda}\int \frac{d^2q}{(2\pi)^2}[|\vec{\phi}_1(\mathbf{q})(1+e^{-i\mathbf{q}\cdot\mathbf{R}})|^2 \\ &\quad -\boldsymbol{\phi}_1(-\mathbf{q})\cdot(\mathbf{A}_{v1}(\mathbf{q}) + \mathbf{A}_{v2}(\mathbf{q})|1+e^{-i\mathbf{q}\cdot\mathbf{R}}|^2] \\ &\quad -2E_{lv} \\ &= \frac{\phi_0^2}{4\pi^2}\int \frac{J_0(qR)}{1+\Lambda q}dq \\ &= \frac{\phi_0^2}{8\pi\Lambda}[\mathbf{H}_0(\frac{R}{\Lambda}) - N_0(\frac{R}{\Lambda})]\,. \end{aligned} \tag{2.43}$$

In the last step we have used the formula [49]:

$$\int_0^\infty \frac{1}{x+z}J_0(cx)dx = \frac{\pi}{2}[\mathbf{H}_0(cz) - N_0(cz)]\,, \tag{2.44}$$

where $\mathbf{H}_0(x)$ is the zeroth Struve function, and $N_0(x)$ is the zeroth Neumann function. The asymptotic form of the interaction energy (2.43) is as follows:

$$V_{ll}(R) = \begin{cases} \frac{\phi_0^2}{4\pi^2\Lambda}\ln\frac{\Lambda}{R} & (d \ll R \ll \Lambda) \\ \frac{\phi_0^2}{4\pi^2 R} & (R \gg \Lambda)\,. \end{cases} \tag{2.45}$$

Eq. (2.37) can be solved by the same method for any number of layers, though calculations become more cumbersome. However, in the region $R \gg Nd$ Eq. (2.37) can be solved quite easily. The vector potential of a pancake vortex, identical at all

layers read:

$$\mathbf{A}_{v1}(\mathbf{q}) = \cdots = \mathbf{A}_{vN}(\mathbf{q}) = \frac{i\phi_0 \hat{z} \times \hat{q}}{q(N + 2\Lambda q)} \,. \tag{2.46}$$

Eq. (2.46) allows to calculate the magnetic field, the current, and the interaction energy. Specifically, the single linear self-energy and the interaction energy of two linear vortex for an N multilayer superconductor are:

$$E_{lv} = \frac{N\phi_0^2}{16\pi^2\Lambda} \ln \frac{\Lambda}{\xi} \,, \tag{2.47}$$

$$V_{ll}(R) = \begin{cases} \frac{N\phi_0^2}{8\pi^2\Lambda} \ln \frac{\Lambda}{R} & (Nd \ll R \ll \Lambda) \\ \frac{\phi_0^2}{4\pi^2 R} & (R \gg \Lambda) \,. \end{cases} \tag{2.48}$$

We see that the energy of a single linear vortex in a N-layers superconducting system is proportional to the number of layers N. The interaction energy between two linear vortex is N times stronger than the corresponding form for two Pearl vortex at a short distance if we replace Λ by λ_e, but at a long distance, the interaction energy has the same form as that for the Pearl vortex.

Next, we discuss ferromagnetic textures in a multilayer system. We assume that the superconducting and ferromagnetic layers form very thin bi-layers separated by a finite distance d. The London-Pearl equation for the vector potential $\mathbf{A}_m$ induced by the magnetic layers and screened by the SC layers is:

$$\begin{aligned} &-\Delta \mathbf{A}_m(\boldsymbol{\rho}, z) + \frac{1}{\Lambda} \sum_n \delta(z - z_n) \mathbf{A}_m(\boldsymbol{\rho}, z) \\ &= 4\pi \sum_n \nabla \times [\mathbf{m} \delta(z - z_n)] \,. \end{aligned} \tag{2.49}$$

Comparing it with Eq. (2.34), we find that they become identical if we replace $i\phi_0 \hat{z} \times \hat{q}/q$ by $i4\pi m_q \Lambda \hat{z} \times \mathbf{q}$ after Fourier-transform. Therefore, it is straightforward to obtain the result for the magnetic vector potential from the vector potential induced by vortex. The Fourier-transform of the vector potential at each layer produced by

an ferromagnetic texture, identical in each plane, reads:

$$\mathbf{A}_{m1}(\mathbf{q}) = \cdots = \mathbf{A}_{mN}(\mathbf{q}) = \frac{i4\pi\Lambda m_q \hat{z} \times \mathbf{q}}{N + 2\Lambda q}\,. \tag{2.50}$$

Eqs. (2.46) and (2.50) allow to calculate the interaction energy of ferromagnetic textures and vortex-ferromagnet interaction energy for a given magnetic texture.

Let us consider the spontaneous stripe vortex-domain structure in a N-layer ferromagnet-Superconductor, assuming as before that both the stripe width L'_s and the distances between vortex are much larger than Λ. As we mentioned before, the interaction energy between two linear vortex has the same form as in a single layer, but the energy of a linear vortex is proportional to N. The vortex-ferromagnet interaction energy is also proportional to N. That means that the condition required for spontaneous formation of vortex and antivortex remains the same as for the bilayer:

$$m\phi_0 > \epsilon_v^l\,, \tag{2.51}$$

where $\epsilon_v^l = \frac{\phi_0^2}{16\pi^2\Lambda}\ln\frac{\Lambda}{\xi}$. A consideration similar to that of Sec. II and II leads to following results. The equilibrium domain width for a N-layer is:

$$L'_s = \frac{\Lambda}{4}\exp(\frac{\tilde{\epsilon}_{dw}}{4N\tilde{m_l}^2} - C + 1)\,, \tag{2.52}$$

where $\tilde{m}_l = m - \epsilon_v^l/\phi_0$. The factor $1/N$ in the exponent (2.52) significantly reduces the domain width. The total width of parallel and antiparallel domains in an external magnetic field (the period of the domain structure) is:

$$L'(B_{ext}) = \frac{2L'_s}{\sqrt{1 - (\frac{L'_s B_{ext}}{2N\pi\tilde{m}_l})^2}}\,. \tag{2.53}$$

The difference of the widths of parallel and antiparallel domains in an external mag-

netic field reads:

$$t' = \frac{2L'}{\pi} \arctan \frac{L' B_{ext}}{4N\pi\tilde{m}_l} \,. \tag{2.54}$$

The critical field at which the stripe structure vanishes follows from Eq. (2.53):

$$B_{ext}^{c\prime} = \frac{2N\pi\tilde{m}_l}{L'_s} \,. \tag{2.55}$$

Note that it increases with the number of layers N. The shift of the transition temperature $\Delta T_c'$ in the multilayer case is:

$$T_c^* - T_c = \frac{64N\pi m^2 e^2}{\alpha m_s c^2} \exp(\frac{-\tilde{\epsilon}_{dw}}{4Nm^2} + C - 1) - N\sqrt{\frac{8\beta m^2}{\alpha^2 d L'_f}} \,. \tag{2.56}$$

Here L'_f is the stripe width for the N-layer consisting only of ferromagnetic films, i.e. without any superconducting film. This length is proportional to a modified exponent: $L'_f \propto \exp(-\epsilon_{dw}/4Nm^2)$, which can be obtained similarly to Eq. (2.53). Thus, the second term in Eq. (2.56) is proportional to $N\exp(-\epsilon_{dw}/8Nm^2)$, whereas the first term is proportional to $N\exp(-\epsilon_{dw}/4Nm^2)$. Even if the second term in equation (2.56) dominates at small N and ΔT_c is negative, it can change sign at larger N provided a following inequality is true: $\frac{2^{9/2}\pi m e^2\sqrt{dl}}{m_s c^2\sqrt{\beta}} \exp(\frac{C-1}{2}) < 1$, where l is the width of the domain wall of ferromagnetic films.

For the case of a few superconducting films with square array of ferromagnetic columnar dots, the shift of the superconducting transition temperature can be readily obtained from the observation that the distance R between two vortices satisfies an inequality $R \ll \Lambda$ near the transition temperature. Then Eq. (2.47) implies that the vortex line energy in a N multilayer system is proportional to N. We see that each term in the Ginzburg-Landau free energy is proportional to N. Therefore, the shift of the transition temperature is the same as that for a single superconducting film with ferromagnetic dots (Eq. (2.32)).

CHAPTER III

CRITICAL CURRENT IN A SUPERCONDUCTING FILM WITH AN ARRAY OF FERROMAGNETIC DOTS

The purpose of this chapter is to study the transport properties of the S film in the presence of a periodic array of F dots at zero external magnetic field. We assume that the interaction between the periodic array of F-dots and the vortex array in the S-film leads to appearance of vortices and antivotices [19, 20, 31]. Erdin [22] and Pokrovsky and Wei [32] studied an S-film with a square array of F-dots, whose magnetic moments are identical and perpendicular to the film assuming only one pair of vortex and antivortex per elementary cell. Although Erdin[22] found that spontaneous symmetry violation is possible in some range of parameters, we will consider for simplicity the less exotic range of parameters, in which symmetry is not violated. In this case each vortex is located under the center of an F-dot and each antivortex is located in the center of elementary square cell formed by 4 F-dots (See Fig. (1)). In the following we first study the anisotropy of the critical current in this system and its dependence on temperature T near T_c. Next, we find the velocity of the antivortices and the induced electric field for the supercurrent directed along the axis (0, 1). We also discuss the Shapiro steps in this system. Finally, we study the critical current for the antiferromagnetic ordering of the F-dots, which can appear if the magnets are soft.

Let us consider a square array of F-dots with a lattice constant a surmounted over an S-film as it is shown in Fig. 1. Each dot is a circular thin disk with a radius R and a constant magnetization m per unit area directed perpendicular to the plane, i.e., along the $\hat{z}$ direction. We assume that the value of m is in the range corresponding to one and only one vortex-antivortex pair per each ferromagnetic dot. As it was

already mentioned, the vortices are located at the centers of the F-dots, whereas the antivortices are located at the centers of elementary square cells formed by the dots.

The energy per unit area of the system is given by Eq.2.28. Since we are interested only in the motion of V, the term u_{mm} is inessential for further consideration. When

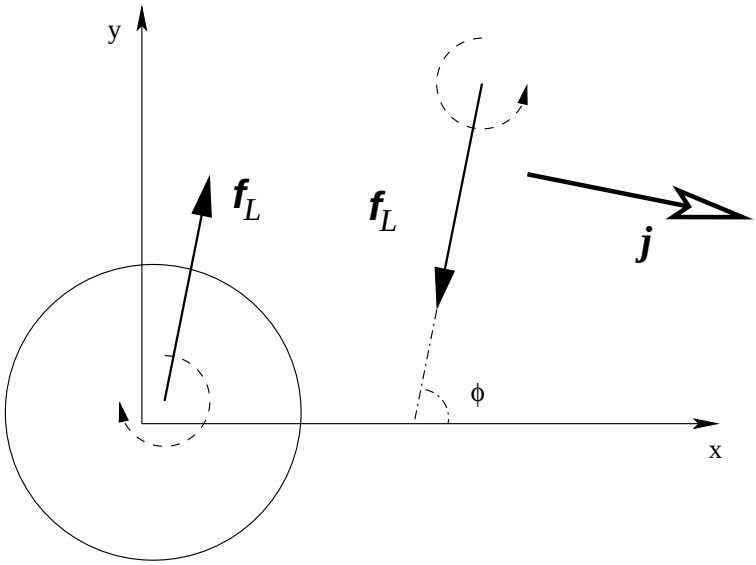

Fig. 3. Schematic representation of the Lorentz forces acting on a vortex and an antivortex. ϕ is the angle between the Lorentz force f_L acting on the vortex and x-axis. The current density j is perpendicular to the f_L.

the transport current **j** flows along the S-film, each vortex or antivortex is subject to the Lorentz force:

$$\mathbf{f}_L = \frac{\Phi_0}{c}\mathbf{j} \times \mathbf{n}\,, \tag{3.1}$$

here $\mathbf{n} = \pm\hat{z}$ is a unit vector perpendicular to the film, "+" and "-" correspond to the vortex and antivortex respectively. The forces acting on the vortex and antivortex have opposite directions (see Fig. 3). At a current lower than critical one, the Lorentz force is balanced by the pinning forces exerted by the ferromagnetic dot array and other vortex and antivortex. The pinning force can be obtained as the gradient of

the energy (2.28) calculated at equilibrium positions $\mathbf{x}_1$ and $\mathbf{x}_2$ of the vortex and antivortex in the unit cell. The driving force increases linearly with the transport current j. Beyond a critical value j_c the Lorentz force acting on the antivortex exceeds the maximum pinning force and the antivortex begin to move. Then, the superconductor transits into the resistive state. We will show later that the pinning force acting on the V is significantly stronger than that acting on the antivortex. Since the pinning force is very strong and the working temperature is low enough even for high-temperature superconductors, we neglect the thermal depinning effect. To describe the action of the transport current we introduce a linear term in the energy Eq. (2.28):

$$U(\mathbf{j}) = U - \frac{1}{a^2}\left[\mathbf{f}_L \cdot (\mathbf{x}_1 - \mathbf{x}_1^0) - \mathbf{f}_L \cdot (\mathbf{x}_2 - \mathbf{x}_2^0)\right] , \tag{3.2}$$

where $\mathbf{x}_1^0 = (0, 0)$ and $\mathbf{x}_2^0 = (a/2, a/2)$ are the initial equilibrium positions of a vortex and an antivortex in the unit cell, respectively, in the absence of the transport current. Generally the Lorenz force is a plane vector $\mathbf{f}_L = f_L(\cos\phi, \sin\phi)$.

To obtain the critical current, we employ a visible picture of the critical current j_c as a value at which the local minimum of energy U vanishes. Employing this criterion, we found the critical current $j_c(\phi)$ for different directions of the current characterized by the angle ϕ as shown in Fig. 4. It has a period $\pi/2$ and possesses reflection symmetry with respect to the lines $\phi = n\pi/4$ (n is an integer). In the absence of the transport current the system of V and dots has a symmetry group $C_{4\mathrm{v}}$. Therefore the angle dependence of the critical current is periodic with a period $\pi/2$ and has the reflection symmetry with reflection planes $x = \pm y$, $x = 0$ and $y = 0$. In the calculation, we chose $\lambda_e = 0.15a$, $R = 0.3a$ and $4\pi^2 mR/\Phi_0 = 20$. A natural unit for the critical current is $\frac{mRc}{20a^2}$ which is equal to $5.0/a(\mu m)$ A/cm. For a typical values $M = 10^2 Gs$, $a = 1\mu$m and $d_s = 50$ nm, the critical current per unit area is about 10^6

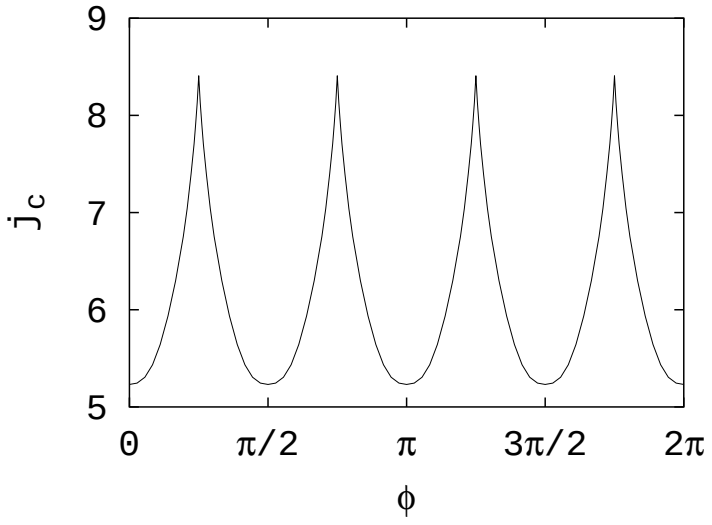

Fig. 4. The critical current j_c vs. angle ϕ. j_c is in the unit of $\frac{mRc}{20a^2}$.

A/cm^2. The minimum of $j_c = 5.2$ occurs at angle $\phi = 0$, $\phi = \pi/2$, etc. The maximal value of j_c is 8.4 occurs at $\phi = \pi/4$, etc. Near the maximal value j_c has sharp peaks. In contrast, it changes smoothly near the minimal values. The pinning force on the line $\phi = \pi/2$ is weaker than that on the line $\phi = \pi/4$. Therefore the critical current along the direction $\phi = \pi/2$ is less than that along the angle $\phi = \pi/4$. From Fig. 3 we see that $j_c(\pi/4)$ is about 1.6 times larger than $j_c(\pi/2)$, although the repulsive force acting on the antivortex is very large when an antivortex goes to the edge of ferromagnetic dots. This is reasonable since the antivortex does not approach the F-dots closely even when the force directed along $\phi = \pi/4$ and it always tries to be far away from ferromagnetic dots. Each ferromagnetic dot strongly attracts the vertex to its center and repels antivortex. Since the vortex is just under the ferromagnetic dot and antivortex is outside the dots, the interaction between the dot and the vertex is much stronger than the interaction between the dots and antivortex. The numerical calculation shows that the maximal pinning force acting to the antivortex is about

0.01 of the maximal pinning force on the vortex. Thus, with a good precision vertex can be assumed to be located at the centers of the F-dots and only antivortex change their positions when an external current is applied.

With the increase of temperature T, as it follows from Eq. (4.6), the energy of the magnetization-vortex interaction becomes small, and thus the pinning force and the critical current j_c drops down. Near T_c this energy can be estimated as follows: $u_{mv} \propto 1/\lambda_e \propto (T_c - T)$ and the critical current $j_c \sim u_{mv}/\xi \propto (1 - T/T_c)^{3/2}$. [50] (we used the well-known formula for superconducting coherence length $\xi(T) = \xi(0)/(1 - T/T_c)^{\frac{1}{2}}$).

Now we are in a position to calculate the resistivity of the S-film when the current exceeds its critical value. When an antivortex moves, there are three forces acting on it, namely, the driving Lorentz force, the pinning force and the friction force. We neglected the Hall force here because it is usually very small.[43] For simplicity, we restrict ourselves to the case of the transport current j_d directed along the y-axis. Then, all the three forces are directed along the x-axis and the antivortex move in the same direction. As it was discussed earlier, the pinning force acting to the vortex under the dot is much stronger than that acting on the antivortex outside, so there is an interval of the currents exceeding the critical, but still small enough to ensure that vortices are pinned at the centers of the dots. From Eq. (2.28) the pinning force acting on a moving antivortex is:

$$\begin{aligned} f_x &= \frac{\Phi_0^2}{\pi a^4} \sum_{n>0,s} \frac{\frac{4\pi^2 mR}{\Phi_0} J_1(\frac{2\pi R}{a}\sqrt{n^2+s^2}) - 1}{\sqrt{n^2+s^2}(1+\frac{4\pi\lambda_e}{a}\sqrt{n^2+s^2})} \\ &\quad \cdot n(-1)^s \sin\frac{2\pi n x}{a} \\ &\approx A\sin(\frac{2\pi x}{a})\,. \end{aligned} \tag{3.3}$$

Here we neglected the terms in the series with $n \geq 2$ since the $n = 2$ term is about

10 times less than the first term and $n \geq 3$ terms are much smaller, etc. This approximation becomes even more accurate if the square lattice dots is replaced by a rectangular lattice dots as in the work of Ref.[25] A is a coefficient given by the following expression:

$$A = \frac{2\Phi_0^2}{\pi a^4} \sum_s \frac{\frac{4\pi^2 mR}{\Phi_0} J_1(\frac{\pi R}{a}\sqrt{1+s^2}) - 1}{\sqrt{1+s^2}(1+\frac{4\pi\lambda_e}{a}\sqrt{1+s^2})}(-1)^s \,. \tag{3.4}$$

The equation of motion for an unpinned antivortex is:

$$\eta \frac{dx}{dt} + A\sin(\frac{2\pi x}{a}) = \frac{\Phi_0}{c} j_d \,, \tag{3.5}$$

where $\eta = \Phi_0 H_{c2} d/c^2 \rho_n$ is the Bardeen-Stephen drag coefficient, H_{c2} is the upper critical magnetic field, c is the speed of light and ρ_n is the normal-state resistivity of the S-film, and j_d is the driving DC current. Solving Eq. (3.5), we obtain the velocity of an antivortex:

$$v = \frac{dx}{dt} = \frac{c\eta a^2 \omega^2}{4\pi^2 \Phi_0 (j_d - j_{c0}\cos\omega t)} \tag{3.6}$$

Here $\omega = 2\pi\Phi_0\sqrt{j_d^2 - j_{c0}^2}/ca\eta$ and $j_{c0} = cA/\Phi_0$. We chose $t = 0$ coinciding with the location of the maximum of v. When $j_d < j_{c0}$, ω becomes an imaginary number and v is damping. Hence j_{c0} is the critical current along the x direction. The value ω increases with j_d: $\omega \propto j_d$ when $j_d \gg j_{c0}$. Eq. (3.6) implies that the velocity v is periodic function of time with the period $T = 2\pi/\omega$. Thus the average velocity is

$$\bar{v} = \frac{a}{T} = \frac{a\omega}{2\pi} \,. \tag{3.7}$$

The Fourier-components of the velocity are:

$$v_{n\omega} = \frac{1}{T}\int_0^T v(t) e^{in\omega t} dt = \frac{a\omega}{2\pi}\left(\frac{j_d - \sqrt{j_d^2 - j_{c0}^2}}{j_{c0}}\right)^n \,. \tag{3.8}$$

When j_d is very close to j_{c0} the frequency ω approaches zero. To the first order

in ω, $v_{n\omega} \approx a\omega/2\pi$ independently on n. In an opposite asymptotic region of large transport currents $j_d \gg j_{c0}$ the Fourier-components of velocity decay rapidly with the n increasing: $v_{n\omega} \approx \Phi_0 j_{c0}^n / c\eta 2^n j_d^{n-1}$. Employing the Faraday relation $\boldsymbol{E} = \frac{1}{c}\boldsymbol{B} \wedge \boldsymbol{v}$ we find that the average induced electric field is $\bar{E} = \omega\Phi_0/2\pi ca$ and the Fourier-transform of the induced electric field is $E_{n\omega} = \Phi_0 v_{n\omega}/ca^2$, which approximately are equal to $\Phi_0\omega/2\pi ca$ when j_d is close to j_{c0} and $\Phi_0^2 j_{c0}^n/\eta c^2 a^2 2^n j_d^{n-1}$ when $j_d \gg j_{c0}$. The average Ohmic loss is $P = \eta\bar{v}^2 = \Phi_0^2(j_d^2 - j_{c0}^2)/c^2\eta$. Finally, we present the formula for the resistivity $\rho(n\omega)$:

$$\begin{aligned} \rho(n\omega) &= \frac{dE_\omega}{dj_d} \\ &= \frac{\Phi_0^2(j_d - n\sqrt{j_d^2 - j_{c0}^2})}{c^2 a^2 \eta \sqrt{j_d^2 - j_{c0}^2}} \left(\frac{j_d - \sqrt{j_d^2 - j_{c0}^2}}{j_{c0}} \right)^n . \end{aligned} \tag{3.9}$$

In the work[25] the authors show that Shapiro steps can appear when the periodic pinning array is rectangular when the pinning potentials are modeled by attractive parabolic wells. Below we show that the Shapiro steps can also appear for the pinning potential calculated consequently in the framework of the London magneto-static equations (see Eq.(4.6)). Thus, our results are valid not only qualitatively, but also quantitatively. Let us assume that both an AC current j_a and a DC current j_d are applied along the y direction. Eq. (3.5) becomes:

$$\eta \frac{dx}{dt} + A \sin\left(\frac{2\pi x}{a}\right) = \frac{\Phi_0}{c} j_d + \frac{\Phi_0}{c} j_a \cos(\omega_0 t) , \tag{3.10}$$

where ω_0 is the frequency of the AC current. Eq (3.10) has the same structure as Eq. (4) in the Ref.[25]. Hence we can follow their arguments to obtain the range Δj_d of the DC current j_d for which the motion of antivortex can be locked to the nth

harmonic of AC current:

$$\Delta j_d = \frac{2cA}{\Phi_0} \left| J_n \left(\frac{2\pi\Phi_0 j_a}{c\eta\omega_0 a} \right) \right| , \tag{3.11}$$

where $J_n(x)$ is the Bessel function of the order n.

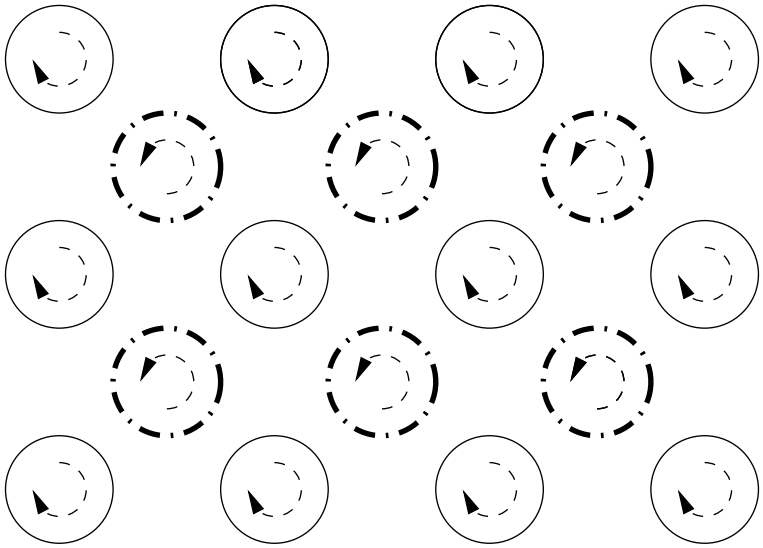

Fig. 5. Schematic view of the antiferromagnetic ordered array of ferromagnetic dots and induced vortices and antivortices. Solid circles denote the ferromagnetic dots with positive magnetic moments, dashed circles denote the ferromagnetic dots with negative magnetic moments. The arrows indicate vortex and antivortex respectively.

Finally, we consider the antiferromagnetic ordering of the ferromagnetic dot array. It means that the direction of magnetic moment of each dot is opposed to those of its nearest neighbors as it is shown in Fig. 5. For the reason mentioned before, at a definite value of the product of magnetization m and the radius R, a vortex or antivortex appears under the center of each F-dot depending on the magnetization sign of the dot. The resulting system has the periodicity of a square centered lattice with the lattice constant $2a$. We calculate the critical current in this struc-

ture. Under the influence of the transport current j both vortex and antivortex move away from the centers of the dots. Let $\mathbf{x}_1$ and $\mathbf{x}_2$ be the positions of the vortex and antivortex, respectively, in a primitive unit cell when current is applied to the system. To obtain the critical current it is possible to modify slightly the approach which we used for the dots with identical magnetic moments by replacing $m_{z\mathbf{G}}$ by $m_{z\mathbf{G}}(1-(-1)^{n+s})$ in Eq. (4.6) and considering the displacements of vortex and antivortex on the same footing. In our numerical calculation all the parameters are chosen the same as before. At zero temperature the results are as follows: $j_c(\pi/4) = 188.2$ and $j_c(\pi/2) = 182.8$ with unit we mentioned before. Anisotropy is very small: $(j_c(\pi/4) - j_c(\pi/2))/j_c(\pi/4) \approx 0.03$. These critical currents are quite large and they are by the order of magnitude $\sim$ 2000(A/cm). For the thickness of the S-film 50 nm, the critical current per unit area j_c/d_s is about 10^8 A/cm^2. This value may be even larger than the depairing current. The critical current j_c is a monotonically decreasing function of temperature. Near T_c we have the same relationship $j_c \propto (1 - T/T_c)^{3/2}$ as before.

CHAPTER IV

SPONTANEOUS VORTEX CREATION IN A SUPERCONDUCTING FILM BY FERROMAGNETIC DOTS

Spontaneous vortices due to the interaction between a superconducting film and an ultra-thin ferromagnetic dot with in-plane magnetization has been discussed in Ref.[20]. We here focus on the interaction between an superconducting film and an array of such dots. First, we show why a large in-plane ferromagnetic dot produces vortices more easily than by using a ferromagnetic dot whose magnetization is normal to the superconducting film; Next, we argue why the system with spontaneous vortices and antivortices has the same symmetry as the original array dot with in-plane magnetization and why the symmetry may be broken if the ferromagnetic dots have their magnetization perpendicular to the superconducting film. Then the phase diagrams for the spontaneous vortices for a square array of circular and square ferromagnetic dots are presented. Finally, we consider a square ferromagnetic dot at the boundary of a semi-infinite superconducting film and study the relationship among the dot's magnetization m, the distance a from dot's center to the superconducting boundary, and the side length of the dot.

Ferromagnetic dots with magnetization perpendicular to the superconducting film are generally discussed for spontaneously vortices due to the interaction between a superconducting film and ferromagnetic dots. In this case the interaction energy ϵ_{mv} between a superconducting film and a ferromagnetic dot is at most $-m\Phi_0$ (here $m = Md_m$. M is the magnetization of the bulk ferromagnetic film and d_m is the thickness of the ferromagnetic film).[20] To satisfy the spontaneous condition $\epsilon_v - m\Phi_0 < 0$, it usually requires the temperature T is close to T_c so that ϵ_v, which is proportional to $1-T/T_c$, is less than $m\Phi_0$. $\Phi_0 = hc/2e$ is the flux quantum, and ϵ_v is the single vortex

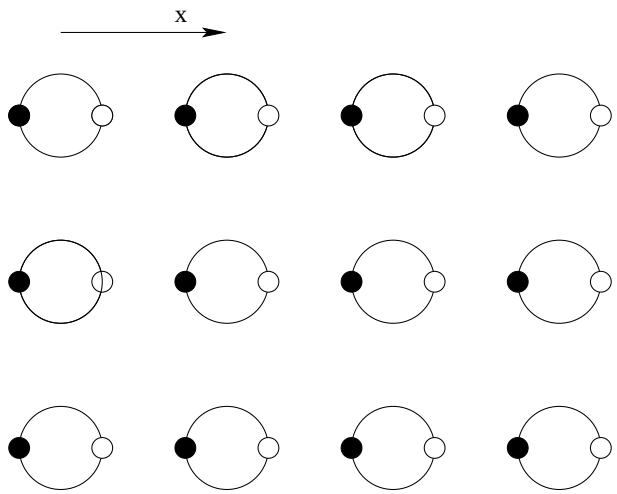

Fig. 6. Schematically show the geometry of the array of ferromagnetic dots on a superconducting film. The the large circles without colors represent thin ferromagnetic dots with a constant magnetization along the $\hat{x}$ direction. The small black circles represent vortices and the small white circles represents antivortices respectively.

energy. We here mainly discuss ferromagnetic dots with in-plane magnetization in which the magnetization of the dot is parallel with the superconducting film as Fig. 6 shown. The characteristics of in-plane magnetization can be shown as follows: For a single vortex at the origin of an superconducting film which is located at $z = 0$, the in-plane magnetic field due to it is:[51]

$$\mathbf{b}_v^{\parallel}(\mathbf{r}, z = 0^{\pm}) = \pm\hat{r}\frac{\Phi_0}{2\pi}\int_0^{\infty}\frac{qJ_1(qr)}{1 + 2q\lambda_e}dq\,, \tag{4.1}$$

where $0^{\pm}$ indicates the position just above or below the superconducting film; $\boldsymbol{r}$=(x, y) is the 2-dimensional coordinate and $J_1(x)$ is the Bessel function. At large distance $r \gg \lambda_e$, i.e. $q \ll \lambda_e^{-1}$, the above equation becomes

$$\mathbf{b}_v^{\parallel}(\mathbf{r}, z = 0^{\pm}) = \pm\frac{\Phi_0}{2\pi}\frac{\mathbf{r}}{r^3}\,. \tag{4.2}$$

Thus, if we consider an ferromagnetic dot with the magnetization parallel to the $\hat{x}$ direction and with so size large that it occupies the half plane $x > 0$, the interaction energy between the vortex and the ferromagnetic dot is (see Eq. (4.11))

$$\epsilon_{mv} = -\int \mathbf{m} \cdot \mathbf{b}_v^{\parallel} d^2\mathbf{r} \sim -\frac{m\Phi_0}{\pi} \ln R/\lambda_e \,. \tag{4.3}$$

It is divergent as $\ln R$ for $R \gg \lambda_e$. Thus, the condition $\epsilon_v + \epsilon_{mv} < 0$ can be easily satisfied even when ϵ_v is large at $T \ll T_c$ for a finite m. It is easy to check that the most energy favorable configuration is that a vortex appears at the boundary of the half-infinite ferromagnetic dot, i.e. at the line $x = 0$. For a finite size ferromagnetic dot, we can expect that another antivortex will appear at the opposite boundary of the ferromagnetic dot.

Now we study a 2D square array of ferromagnetic dots with in-plane magnetization on the superconducting film as Fig. 1 shown. The energy per unit area of the two dimensional system about vortices is:[20]

$$u = u_{vv} + u_{mv} \,, \tag{4.4}$$

here u_{vv} is the energy of vortex and u_{mv} is the interaction energy between vortex and ferromagnetic dots. Each term of Eq. (4.4) can be given respectively as follows:

$$u_{vv} = \frac{1}{A}\sum_{\mathbf{G}} \left[\frac{\epsilon_0}{2\pi} |(\nabla\varphi)_{\mathbf{G}}|^2 - \frac{\Phi_0}{16\pi^2\lambda_e} \nabla\varphi_{\mathbf{G}} \cdot \mathbf{a}^v_{-\mathbf{G}} \right] , \tag{4.5}$$

$$u_{mv} = -\frac{1}{A}\sum_{\mathbf{G}} \left[\frac{\Phi_0}{16\pi^2\lambda_e} (\nabla\varphi)_{\mathbf{G}} \cdot \mathbf{a}^m_{-\mathbf{G}} + \frac{1}{2}\mathbf{b}^v_{\mathbf{G}} \cdot \mathbf{m}_{-\mathbf{G}} \right] , \tag{4.6}$$

where $A = a^2$ is the area of the unit cell; a is the lattice constant of the square array

and $\epsilon_0 = \Phi_0^2/16\pi^2\lambda_e$. The singular phase gradient due to vortices is

$$(\nabla\varphi)_{\mathbf{G}} = \frac{i2\pi}{A}\frac{\mathbf{G}\times\hat{z}}{G^2}F_{\mathbf{G}}\,, \tag{4.7}$$

where $F_{\mathbf{G}} = \sum_i n_i e^{-i\mathbf{G}\cdot\mathbf{r}_i}$ is the structure factor of vortex and n_i, $\mathbf{r}_i$ indicate the vorticity and the position of the ith vortex respectively. $\mathbf{a}$ and $\mathbf{b}$ are the vector potential and the magnetic field at the plane $z = 0$ respectively. The superscripts m and v on $\mathbf{a}$ and $\mathbf{b}$ indicate that they are produced by magnetization and vortices respectively. In the following discussion, we specify that the direction of the magnetization $\mathbf{m}$ of the ferromagnetic dot is along the $\hat{x}$ direction, i.e. one of the axes of the square array of the ferromagnetic dot in the plane. From Ref.[20] we have

$$a_{\mathbf{G}}^{m\perp} = -\frac{4\pi\lambda_e G}{1+2\lambda_e G}m_{\mathbf{G}}^{\parallel}\,, \tag{4.8}$$

and the magnetic field due the in plane magnetization on the plane $z = 0$ is

$$\mathbf{b}_{\mathbf{G}}^{m\parallel} = -2\pi\left(1+\frac{1}{1+2\lambda_e G}\right)m_{\mathbf{G}}^{\parallel}\mathbf{G}\,. \tag{4.9}$$

The magnetic field due to vortices is

$$\mathbf{b}_{\mathbf{G}}^{v\parallel} = -\frac{i\Phi_0 F_{\mathbf{G}}}{G(1+2\lambda_e G)}\mathbf{G}\,. \tag{4.10}$$

"$\perp$" and "$\parallel$" show the direction along the $\hat{z}\times\hat{\mathbf{G}}$ and $\hat{\mathbf{G}}$ respectively. Substitute Eqs.(4.7)-(4.10) into Eq. (4.6) and we find that two terms of it are equal to each other. Then Eq. (4.6) becomes

$$u_{mv} = -\frac{1}{A}\sum_{\mathbf{G}}\mathbf{b}_{\mathbf{G}}^{v}\cdot\mathbf{m}_{-\mathbf{G}}\,. \tag{4.11}$$

We can obtain the same result as Eq. (4.11)for the case of ferromagnetic dots with magnetization perpendicular to the superconducting film. The physical meaning of the interaction between vortices and ferromagnetic dots becomes transparent now: it

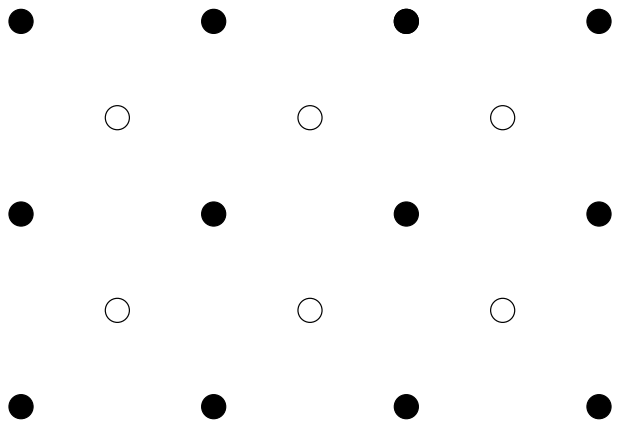

Fig. 7. Schematic representation the unstable lattice structure for the vortices and antivortices. The black circles correspond to vortices and the white circles correspond to antivortices respectively.

is the ferromagnetic dots interacted by the magnetic field of vortices. When energy (4.4) $u < 0$, the vortices is energetically favored to appear in the system. It has been proved that the vortices and antivortices must appear in pairs so that the net magnetic field is zero in Ref. [21]. Denote the positions of the vortex and antivortex by $\mathbf{r}_i^v$ and $\mathbf{r}_i^{av}$ in each pair respectively. the pairs are labeled by $i = 1, 2, \cdots$. If we make the following operation for each pair: $\mathbf{r}_i^v \leftrightarrow -\mathbf{r}_i^{av}$, the energy (4.4) is invariant. Then, it can be shown that $\mathbf{r}_i^{av} = -\mathbf{r}_i^v$ for the minimum energy configuration of the system. In addition, if we make the following transformation: $\mathbf{r}_i^v \rightarrow \tilde{\mathbf{r}}_i^v$ and $\mathbf{r}_i^{av} \rightarrow \tilde{\mathbf{r}}_i^{av}$, where $\mathbf{r}^{v,av}$=$(x^{v,av},\ y^{v,av})$ $\tilde{\mathbf{r}}^{v,av}$=$(x^{v,av},\ -y^{v,av})$, the energy (4.4) is also invariant. Thus, the system with vortices and antivortices has the same symmetry as the original ferromagnetic dot lattice, i.e. the image symmetry about the $\hat{x}$ axis.

This symmetry property contrasts with the case of a square array of circular ferromagnetic dots with the magnetization perpendicular to the superconducting film. Refs.[22, 34] numerically showed that the symmetry may be breaking in that case but

the physics for this symmetry broken was not clear. In the following we present the physical picture for it by considering the simplest case in which only one vortex and antivortex spontaneously appear due to the array of ferromagnetic dots. For an antivortex at the origin of a superconducting film, the magnetic field due this antivortex at the superconducting film, $z = 0^+$, is:[51] $B^z(r, 0) = -\Phi_0\lambda_e/(\pi r^3)$ when $r \gg \lambda_e$. Now we assume a ferromagnetic dot is located far way from the antivortex at $r \gg \lambda_e$ and the radius R of the dot satisfies the condition $R \ll r$. Then the interaction energy between the ferromagnetic dot and the antivortex is

$$E_{m-av} = -\int mB^z d^2x' = \frac{m\Phi_0 R^2\lambda_e}{r^3}\,, \tag{4.12}$$

which falls off as $1/r^3$. On the other hand, the interaction energy between a vortex and antivortex at large distance $r \gg \lambda_e$ is:

$$E_{v-av} = -\frac{\Phi_0^2}{4\pi^2 r}\,, \tag{4.13}$$

which falls off as $1/r$. Thus, from Eqs. (4.12) and (4.13) we see that at the large distance $r \gg \lambda_e$, the interaction between the vortex and the antivortex is much larger than the interaction between the antivortex and the ferromagnetic dot. We apply this physic picture to the lattice of vortices and antivortices due the ferromagnetic dot's lattice as Fig. 7 shown. When the lattice constant a is much larger than the effective penetration depth λ_e, and the antivortices initially are located at the centers of each square unit cell, it is obvious that this lattice structure is unstable due to attraction between the two subset lattices of vortices and antivortices. The vortex and the antivortex try to get close to each other in each unit cell until the antivortex is about the distance of λ_e from the ferromagnetic dot because then the repulsion due to ferromagnetic dot balances the attraction between the vortex and antivortex. The critical lattice constant a_c at which the symmetry of the lattice is broken can be

estimated by equating the two energy term Eqs. (4.12) and (4.13), and the result is:

$$a_c = \sqrt{\frac{8\pi^2 m R^2 \lambda_e}{\Phi_0}}\,, \tag{4.14}$$

which is of the same order as the numerical result by Erdin[22]. This simple physical picture can be generalized to the case of multi-pairs of vortices and antivortices.

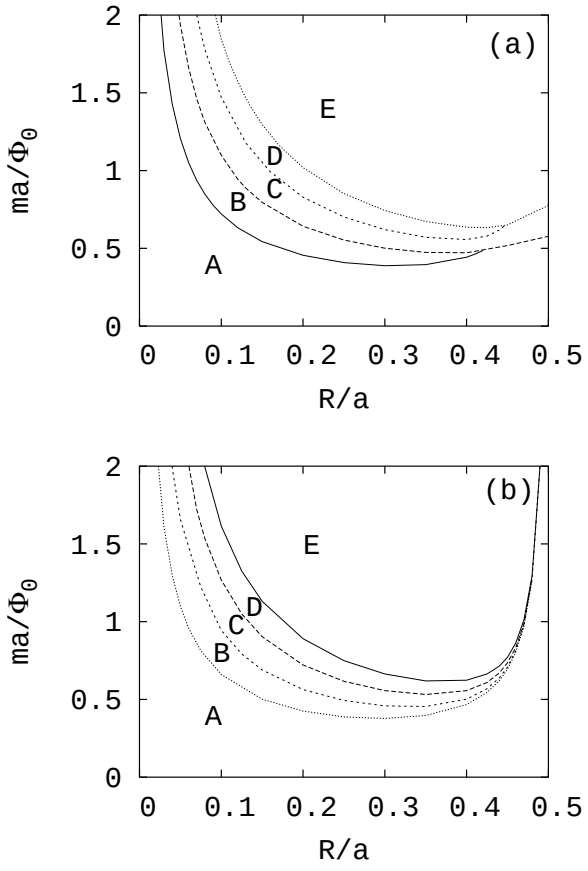

Fig. 8. Fig. (a) is for the case of circular ferromagnetic dot array and Fig. (b) is for the case of square ferromagnetic dot array. In region "A", "B", "C", "D", there are 0, 1, 2, 3 pairs of vortices and antivortices respectively; in region "E", there are more than three pairs vortices and antivortices. R is radius of the circular dots in (a) and the half side length of the square dots in (b) respectively.

We consider each unit cell of the array having just one circular or square ferromagnetic dot with in-plane magnetization along the $\hat{x}$ direction as Fig. 6 shown. For a circular ferromagnetic dot:

$$\mathbf{m} = m\theta(R-\rho)\hat{x}\,, \tag{4.15}$$

where $\theta(x)$ is the step function; R is the radius of the dot. The Fourier component of the dots' array is:

$$m_{\mathbf{G}} = \frac{2\pi m_0 R J_1(GR)}{a^2 G}\hat{x}\,. \tag{4.16}$$

For a square dot:

$$\mathbf{m} = m\theta(x-R)\theta(x+R)\theta(y-R)\theta(y+R)\hat{x}\,, \tag{4.17}$$

where $2R$ is the side length of the square. The Fourier component of the dots' array is:

$$\mathbf{m_G} = \frac{4m\sin G_x R \sin G_y R}{a^2 G_x G_y}\hat{x}\,. \tag{4.18}$$

Substituting Eqs. (4.16) and (4.18) into Eq. (4.11) respectively, and using the condition that the energy (4.4) $u < 0$ for the appearance the spontaneous vortices and antivortices, we can obtain the phase diagram in Fig. 8a for the case of the circular dots and in Fig. 8b for the case of the square dots respectively. We chose $\lambda_e/\xi = 50$ and $\lambda_e/a = 0.3$ in our numerical calculation. In the phase diagram Fig. 8, the regions "A", "B", "C", "D", represent 0, 1, 2, 3 pairs of vortices and antivortices per unit cell respectively; in region "E", there are more than three pairs of vortices and antivortices per unit cell. for $R/a < 0.3$, the phase diagrams of the two cases have very similar structure: with the increase of R/a from 0, the corresponding threshold values m decrease sharply; after $R/a > 0.2$, the threshold values m decrease slowly; when $R/a \sim 0.3 \div 0.4$, the threshold values m have minimum ones. The differences

appear when $R/a > 0.4$. For the circular dots, the first critical line and the second one, and the third and the fourth ones merge together respectively. After that, these line positions increase slowly with R/a. This means that when $R/a \sim 0.5$, there only exist 0, 2, 4, $\cdots$ pairs of vortices and antivortices instead of odd numbers of pairs at some values of m. For the square case, all the critical lines merge together and increase sharply. This means that it is difficult to spontaneously produce vortices when R/a is close to 0.5 for the square case. The positions of the vortices and antivortices are schematically showed in Fig. 9a and 9b for the case of a circular dot array and a square dot array respectively. As the Fig. 9 shows, their positions are located at the boundary of the ferromagnetic dots in the precision of ξ, the smallest length scale in our framework. These most energy favorable positions are due to strong interactions

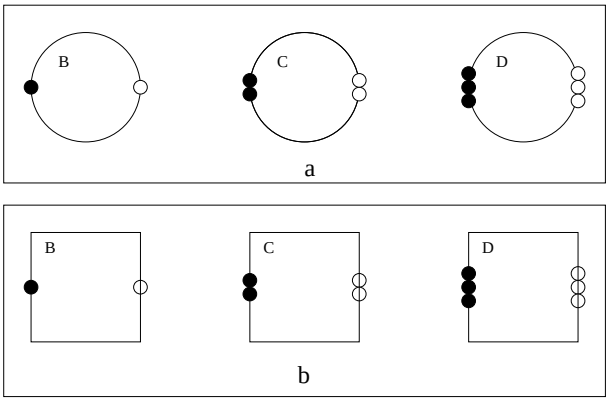

Fig. 9. Schematically show the positions of vortices and antivortices in each unit cell respectively. (a) is for the case of circular ferromagnetic dot array and (b) is for the case of square ferromagnetic dot array. "B", "C", "D" correspond to 1, 2, 3 pairs of vortices and antivortices respectively.

between vortices (antivortices) and ferromagnetic dots. in addition, the positions of each pair of vortex and antivortex have space inversion symmetry about the center of the ferromagnetic dot, and the total system has image symmetry about the $\hat{x}$ axis.

We mention an interesting phenomena in the system, that the vortices and antivortices pairs will annihilate each other when an applied current flows along the $\hat{y}$ direction in the superconducting film and it is beyond the critical value which corresponds to the maximum pining force for vortices and antivortices. That means superconductivity will be maintained until the current is as large as the depairing current.

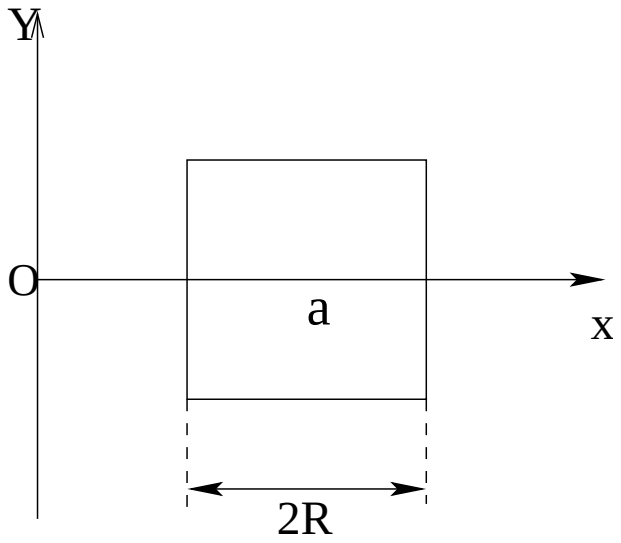

Fig. 10. Schematic representation a square ferromagnetic dot near the boundary of a semi-infinite superconducting film, whose edge is at $x = 0$. The distance between the center of the dot and the boundary of the superconducting film is a. The side length of the square is $2R$.

Lastly, we consider a square ferromagnetic dot with a side length $2R$ near the boundary of a semi-infinite superconducting film, whose edge is at $x = 0$ as Fig. 10 shown. The distance between the center of the dot and the boundary of the superconducting film is a. We concentrate on the conditions for a single spontaneous vortex due to this ferromagnetic dot. From Ref. [22], we know that the energy of a

single vortex near the superconducting boundary is:

$$\epsilon_v = \frac{\Phi_0^2}{16\pi^2\lambda_e}\left[\ln\frac{8\lambda_e}{e^\gamma\xi} - \frac{\pi}{2}\mathbf{\Phi}_0\left(\frac{a}{2\lambda_e}\right)\right], \tag{4.19}$$

here $\gamma = 0.577\ldots$ is the Euler's constant. the interaction energy between a vortex and the ferromagnetic dot is:

$$\epsilon_{mv} = \frac{2\pi m}{c}\int \partial_x G d^2\mathbf{x}\,, \tag{4.20}$$

where the integral domain is the inside of the square dot; The function G has the following form:

$$G(\mathbf{r}) = \frac{c\Phi_0}{16\pi\lambda_e}\left[\mathbf{\Phi}_0\left(\frac{|\mathbf{r}-\mathbf{a}|}{4\lambda_e}\right) - \mathbf{\Phi}_0\left(\frac{|\mathbf{r}+\mathbf{a}|}{4\lambda_e}\right)\right], \tag{4.21}$$

where $\mathbf{\Phi}_0(x) = Y_0(x) - \mathbf{H}_0(x)$, and $\mathbf{H}_0$ and Y_0 are the Struve and the second kind Bessel functions. We present the threshold values $m\lambda_e/\Phi_0$ vs. a/λ_e for the appearance of one single vortex in Figs. 11 by using the same spontaneous condition mentioned before . We choose $\lambda_e/\xi = 50$ in our calculation. From Fig. 10a to 10d, the side length in the unit λ_e is $2R/\lambda_e = 0.67$, 3.34, 13.34, and 33.34 respectively. Because the competition dependending on the position a, between the energy of single vortex and the interaction energy between a vortex and the ferromagnetic dot, we see that for a very small square side, there is a sharp peak in the curve for small a. With the increase of the dot size the peak is relaxed, and at large size it disappears and the threshold values m increase monotonically with a. For $a \gg \lambda_e$, the threshold values of m go to the constant bulk value without any effect due to the edge of superconducting film. With the increase of the size of the dot, the threshold values m decrease. This is consistent with the discussion before. The most energy favorable position for this single vortex is located at the boundary of the dot $(a + R, 0)$.

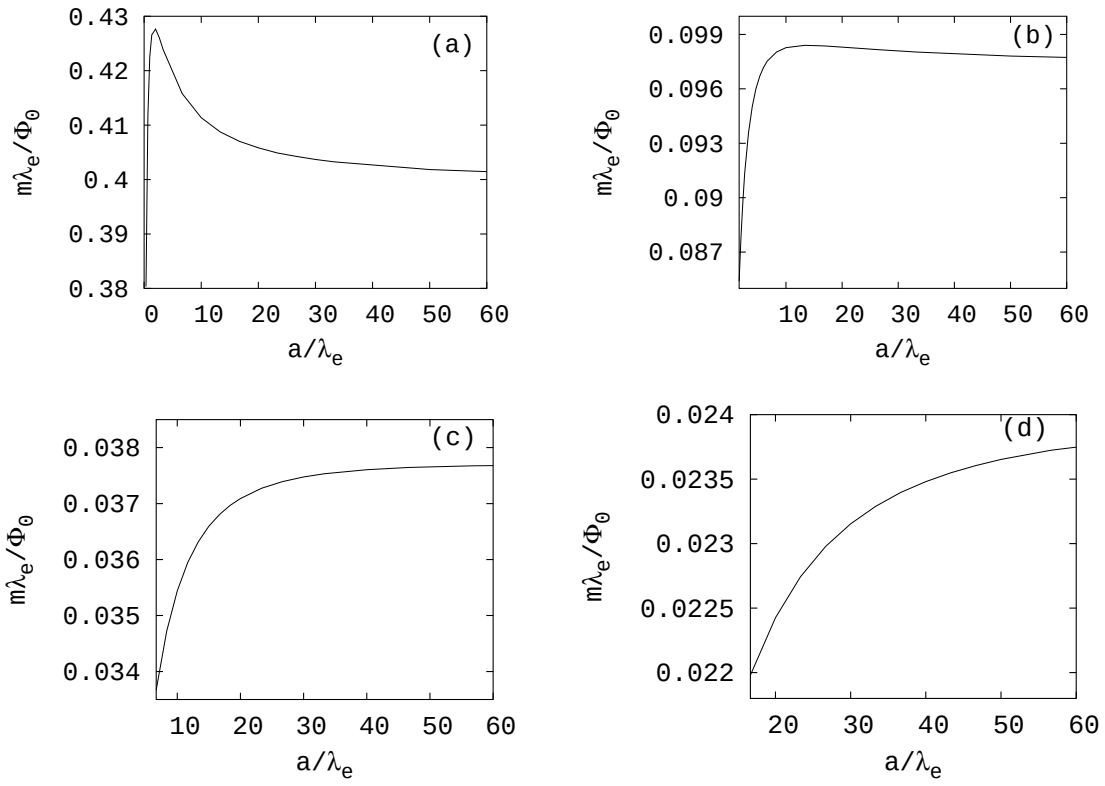

Fig. 11. From (a) to (d), the side length $2R/\lambda_e = 0.67$, 3.34, 13.34, and 33.34 respectively.

CHAPTER V

CONCLUSIONS

In Chapter II, We have studied the characteristics of the superconducting transition and the shift of the transition temperature in heterogeneous ferromagnet-superconductor systems by using the Ginzburg-Landau equation. The competition between combined vortex-domain structure in the ferromagnet-superconductor bilayer and domain structure in the ferromagnetic film with the suppressed superconductivity leads to the first order phase transition. The shift of transition temperature can be positive or negative, depending on the materials used. Typical values of the relative shift $\Delta T_c/T_c$ range from -0.03 to 0.02. It has been demonstrated that the stripe structure must vanish at a very small external magnetic field about 1 to 10 Oersted. Simultaneously the transition temperature may change by the value $\Delta T_c/T_c \sim -0.03$ to 0.02.

In the multilayers case, the critical magnetic field at which the stripe disappears increases with the number of layers, N. The shift of the transition temperature can change sign from negative to positive with increasing N. The reduction of the transition temperature in the superconducting film with ferromagnetic dots may be of the same order of magnitude as in the stripe structure at reasonable values of parameters. In the ferromagnet-superconductor multilayer, this magnitude is the same as that in a single isolated ferromagnet-superconductor bilayer.

The stripes are expected to appear in multilayer samples whose total thickness is much smaller than their lateral size. No stripes will exist in the opposite limiting case. This implies that there must exist a critical value of the ratio of the thickness to the transverse size, at which the stripe structure disappear. The method used here does not allow to calculate this ratio and the corresponding critical behavior.

In chapter III, we have calculated the critical currents j_c for a square lattice of ferromagnetic dots positioned on the superconducting film when the magnetization of each dot is aligned in the same direction perpendicular to the plane with ferromagnetic order or when they alternate. In the first case we predict a significant, though not too large, anisotropy of the critical current. The minimal critical current occurs in the direction along the lines connecting the nearest neighbor dots, whereas the maximum one corresponds to the bisector between the easy current lines. The ratio of the maximum to minimum current is $j_c^{max}/j_c^{min} \approx 1.6$. A typical critical current j_c/d_s in this case is about 10^6 A/cm^2. It decreases with increasing temperature. Near the transition temperature T_c, it is proportional to $(1-T/T_c)^{3/2}$. We have calculated the velocity of the antivortex for the current exceeding its critical value. Since it oscillates, Shapiro steps in the DC resistivity can be observed in this system. For the antiferromagnetic order dots, the calculated anisotropy of the critical current is quite small and its magnitude j_c/d_s is as large as 10^8 A/cm^2. It means that other instabilities, most probably the generation of vortex or phase slip centers near boundaries will generate resistance. These phenomena will also appear in the ferromagnetic ordered case when the transport current is much larger than the critical current for the interstitial antivortex, for example, as large as the critical current for the vortex under ferromagnetic dots. Finally, let us briefly discuss the effects of external magnetic field applied perpendicularly to the superconducting film without a transport current. If $B_{ext} = \Phi_0/a^2$ in the ferromagnetic order array of dots, it either produces an additional vortex or an antivortex per unit cell depending on its sign. A positive field produces an additional vortex under the ferromagnetic dot because the magnetization of each dot is strong and its size is large enough as it was assumed in our work. This statement is confirmed by numerical calculations. A negative field produces an additional antivortex outside of dots due to the same reason. Similar arguments can be applied

to the case of the antiferromagnetic order dot array. One can expect that only vortex remain while the antivortex vanish when the field is very strong and positive. The problems of the upper critical field for such structures and complete phase diagrams including commensurate and incommensurate vortex lattices remain unsolved.

In chapter IV, the interaction between a superconducting film and an array of ferromagnetic dots with in-plane magnetization is discussed. We show that when the size of an ferromagnetic dot is large: $R \gg \lambda_e$, it is easier to spontaneously produce a vortex than those cases in which the magnetization is perpendicular to the superconducting film. We show that the vortex and antivortex positions in each pair have a space inversion symmetry about the center of the ferromagnetic dot, and the total system has image symmetry about the $\hat{x}$ axis. The physical picture as to why the symmetry may be broken is also presented for the case of the magnetization of each ferromagnetic-dot is perpendicular to the superconducting film. The basic reason is that at a large lattice constant $a \gg \lambda_e$, the predominant interaction acting on the antivortex is the long range interaction due to other vortices and antivortices, and the interaction due to ferromagnetic dots can be neglected. This causes the symmetry configuration unstable. In addition, we present the phase diagrams for a square array of circular dots and square dots respectively. At small size $2R \ll a$, their structures is similar; but for large size dots : R closes to $a/2$, their structures are quite different. For the circular dots, the threshold lines appear in pairs, i.e. the lines for the first pair and the line for the second merge together, and the lines for the third pair and the fourth pair merge together. That means only even numbers of vortex is possible when R closes to $a/2$. For square dots, all the threshold lines merge together and increase sharply when R closes to $a/2$. That means no spontaneous vortex and antivortex exist in this limit. Finally, we discuss the condition for the appearance of a vortex for a square ferromagnetic dot located near the boundary of an superconducting film.

The most energy favorable position of this vortex is $(R + a, 0)$, i.e. at the center of one side of the square.

REFERENCES

[1] J. Bardeen, L. Cooper, and J. Schrieffer, Phys. Rev. **108**, 1175 (1957).

[2] L.N. Bulaevskii, V.V. Kuzii, and A.A. Sobyanin, JETP Lett, **25**, 290 (1977).

[3] E.A. Demler, G.B. Arnold, and M.R. Beasley, Phys. Rev. B, **55** 15174 (1997).

[4] A.I. Larkin and Yu. N Ovchinnikov, JETP, **20**, 745 (1965); P. Fulde, and R.A. Ferrel, Phys. Rev. **135**, 550 (1965).

[5] Y. Otani, B. Pannetier, J.P. Nozieres and D. Givord, J. Magn. Magn. Matter. **126**, 622 (1993).

[6] O. Geoffroy, D. Givord, Y. Otani, B. Pannetier and F. Ossart, J. Magn. Magn. Matter. **121**, 233 (1993).

[7] Y. Nozaki, Y. Otani, K. Runge, H. Miyaima, B. Pannetier, J.P. Nozieres and G. Fillion, J. Appl. Phys. **79**, 8571 (1996).

[8] I.K. Marmorkos, A. Matulis and F.M. Peeters, Phys. Rev. B **53**, 2677 (1996).

[9] J. Martin, M. Velez, J. Nogues and I.K. Schuller, Phys. Rev. lett. **79**, 1929 (1997).

[10] D.J. Morgan and J.B. Ketterson, Phys. Rev. Lett. **80**, 3614 (1998).

[11] I.F. Lyuksyutov and V.L. Pokrovsky, Phys. Rev. Lett. **81**, 2344 (1998).

[12] I.F. Lyuksyutov and D.G. Naugle, Modern Phys. Lett. B **13**, 491 (1999).

[13] A. Terentiev, D.B. Watkins, L.E. De Long, D.J. Morgan and J.B. Ketterson, Physica C **332**, 5 (2000).

[14] M.J. Van Bael, L.Van Look, K. Temst, M. Lange, J. Bekaert, U. May, G. Guntherodt, V.V. Moshchalkov and Y. Bruynseraede, Physica C **332**, 12 (2000).

[15] Feldman D.E., Lyuksyutov I.F., Pokrovsky V.L. and V.M. Vinokur, Europhys. Lett. **51**, 110 (2000).

[16] J.E. Santos, E. Frey and F. Schwabl, Phys. Rev. B **63**, 4439 (2001).

[17] L.E. Helseth, Phys. Rev. B **66**, 104508 (2002).

[18] M.A. Kayali, Phys. Lett. A **298**, 432 (2002).

[19] I. E. lyuksyutov and V. L. Pokrovky, Mod. Phys. Lett. B **14**, 409 (2000); I.F. Lyuksyutov and V. Pokrovsky, Phys. Rev. Lett. **81**, 2344(1998).

[20] S. Erdin, M.A. Kayali, I.F. Lyuksyutov, and V.L. Pokrovsky, Phys. Rev. B **66**, 014414 (2002).

[21] S. Erdin, I.F. Lyuksyutov, V.L. Pokrovsky, V.M. Vinokur, Phys. Rev. Lett. **88**, 017001 (2002).

[22] S. Erdin, Physica C **391**, 140 (2003).

[23] J.I. Martín, M. Vélez, A. Hoffmann, I.K. Schuller, and J.L. Vicent, Phys. Rev. Lett. **83**, 1022(1999).

[24] J.I. Martín and M. Vélez, A. Hoffmann, I.K. Schuller, J.L. Vicent, Phys. Rev. B **62**, 9110 (2000).

[25] C. Reichhardt, R.T. Scalettar, G.T. Zimányi, and N. Grønbech-Jensen, Phys. Rev. B **61**, R11914 (2000).

[26] Y. Jaccard, J.I. Martín, M.C. Cyrille, M. Vélez, J.L. Vicent, and I.K. Schuller, Phys. Rev. B **58**, 8232 (1998).

[27] Y. Fasano, J.A. Herbsommer, F. de la Cruz, F. Pardo, P.L. Gammel, E. Bucher and D.J. Bishop, Phys. Rev. B **60**, R15047 (1999).

[28] A. Terentiev, D.B. Watkins, L.E. De Long, L.D. Cooley, D.J. Morgan and J.B. Ketterson, Phys. Rev. B**61**, R9249 (2000).

[29] L. Van Look, E. Rosseel, M.J. Van Bael, K. Temst, V.V. Moshchalkov, and Y. Bruynseraede, Phys. Rev. B **60**, R6998 (2000).

[30] I.F. Lyuksyutov, V.L. Pokrovsky, Advances in Physics, **54**, 67 (2005) .

[31] M.A. Kayali, Phys. Lett. A **298**, 432 (2002); Phys. Rev. B **69**, 012505 (2004); M.A. Kayali, V.L. Pokrovsky, Phys. Rev. B **69**, 132501 (2004).

[32] V.L. Pokrovsky and H. Wei, Phys. Rev. B **69**, 104530 (2004).

[33] H.Wei, Phys. Rev. **71**, 12514(2005).

[34] D.J. Priour, Jr. and H.A. Fertig, Phys. Rev. Lett. **93**, 57003 (2004).

[35] The renormalized energy of vortices is equal to $\tilde{\epsilon}_v = \epsilon_0 - m\phi_0$ instead of $\tilde{\epsilon}_v = \epsilon_0 - \frac{3}{2}m\phi_0$ found in [21]). This leads to a change of the domain width L and energy U (Eqs. (18) and (19) in Ref. [21]). The corrected values are given by Eqs. (2.1) and (refLs) of this article.

[36] Y. Yafet and E.M. Gyorgy, Phys. Rev. B **38**, 9145 (1988).

[37] B. Kaplan and G.A. Gehring, J. Magn. Magn. Matter. **37**, 111 (1993).

[38] R. Allenspach and A. Bischof, Phys. Rev. Lett. **69**, 3385 (1992); R. Allenspach, J. Magn. Magn. Matter. **129**, 160 (1994).

[39] O. Portmann, A. Vaterlaus and D. Pescia, Nature, **422**, 701 (2003).

[40] A.B. Kashuba and V.L. Pokrovsky, Phys. Rev. Lett. **70**, 3155(1993); A. Abanov, V. Kalatsky and V.L. Pokrovsky, Phys. Rev. B **51**, 1023 (1995).

[41] M. Tinkham, *Introduction to Superconductivity*, 2nd ed. (Mc-Graw-Hill, New York, 1996).

[42] A.A. Abrikosov, Zh. Eksp. Teor. Fiz. **32**, 1442 (1957) [Sov. Phys. JETP. **5**, 1174 (1957)].

[43] G. Blatter, M.V. Feigel'man, V.B. Geshkenbein, A.I. Larkin, V.M. Vinokur, Rev. Mod. Phys. **66**, 1125 (1994).

[44] J.R. Clem, Phys. Rev. B **43**, 7837 (1991).

[45] M. Houzet, A. Buzdin, and M.I. Kulić, Phys. Rev. B **64**, 184501 (2001).

[46] R.G. Mints, V.K. Kogan, and J.R. Clem, Phys. Rev. B **61**, 1623 (2000).

[47] K.B. Efetov, Zh. Eksp. Teor. Fiz. **76**, 1781 (1979) [Sov. Phys. JETP **49**, 905 (1979)].

[48] K.H. Fischer, Physica C **178**, 161 (1991).

[49] A.P. Prudnikov, Yu.A. Brychkov, O.I. Marichev, *Integrals and Series*, Vol.**2** (Gordon and Breach Science Publishers, New York, 1986).

[50] P.G. de Gennes, *Superconductivity of Metals and Alloys* (Addison-Wesley, New York, 1989).

[51] A.A. Abrikosov, *Fundamentals of the Theory of metals*, (North Holland,The Nethelands,1988).

[52] V.G. Kogan, Phys. Rev. B **49**, 15874 (1994).

APPENDIX A

METHOD

The the basic method[20] used in this thesis is given here. The total energy of a stationary FM-SC system reads

$$U = \int [\frac{\mathbf{B}^2}{8\pi} + \frac{m_s n_s \mathbf{v}_s^2}{2} - \mathbf{B} \cdot \mathbf{M}] dV. \tag{A.1}$$

where $\mathbf{B}$ is the magnetic induction, $\mathbf{M}$ is the magnetization, n_s is the density of SC electrons, m_s is their effective mass and $\mathbf{v}_s$ is their velocity. It is assumed that the SC density n_s and the magnetization $\mathbf{M}$ to be separated in space. We also assume that the magnetic field $\mathbf{B}$ and its vector-potential $\mathbf{A}$ asymptotically approaches zero at infinity. After the static Maxwell equation $\nabla \times \mathbf{B} = \frac{4\pi}{c}\mathbf{j}$, and $\mathbf{B} = \nabla \times \mathbf{A}$ are employed, the magnetic field energy can be transformed as follows:

$$\int \frac{\mathbf{B}^2}{8\pi} dV = \int \frac{\mathbf{j} \cdot \mathbf{A}}{2c} dV. \tag{A.2}$$

The current $\mathbf{j}$ can be represented as a sum: $\mathbf{j} = \mathbf{j}_s + \mathbf{j}_m$ of the SC and magnetic currents, respectively:

$$\mathbf{j}_s = \frac{n_s \hbar e}{2m_s}(\nabla\varphi - \frac{2\pi}{\phi_0}\mathbf{A}), \tag{A.3}$$

$$\mathbf{j}_m = c\nabla \times \mathbf{M}. \tag{A.4}$$

We separately consider the contributions from magnetic and SC currents to the integral (A.2), starting with the integral:

$$\frac{1}{2c}\int \mathbf{j}_m \cdot \mathbf{A} dV = \frac{1}{2}\int (\nabla \times \mathbf{M}) \cdot \mathbf{A} dV. \tag{A.5}$$

Integrating by parts and neglecting the surface term again, we arrive at

$$\frac{1}{2c}\int \mathbf{j}_m \cdot \mathbf{A} dV = \frac{1}{2}\int \mathbf{M} \cdot \mathbf{B} dV. \tag{A.6}$$

We have omitted the integral over a distant surface:

$$\oint (\mathbf{n} \times \mathbf{M}) \cdot \mathbf{A} dS. \tag{A.7}$$

Such an omission is justified if the magnetization is confined to a limited volume.

We next consider the contribution of the SC current $\mathbf{j}_s$ to the integral (A.2). In the gauge-invariant Eq.(A.3), φ is the phase of the SC carriers wave-function. Note that the phase gradient $\nabla\varphi$ can be incorporated in $\mathbf{A}$ as a gauge transformation. The exception is vortex lines, where φ is singular. We use the equation (A.3) to express the vector potential $\mathbf{A}$ in terms of the supercurrent and the phase gradient:

$$\mathbf{A} = \frac{\phi_0}{2\pi}\nabla\varphi - \frac{m_s c}{n_s e^2}\mathbf{j}_s. \tag{A.8}$$

Plugging Eq.(A.8) into Eq.(A.2), we find

$$\frac{1}{2c}\int \mathbf{j}_s \cdot \mathbf{A} dV = \frac{\hbar}{4e}\int \nabla\varphi \cdot \mathbf{j}_s dV - \frac{m_s}{2n_s e^2}\int j_s^2 dV. \tag{A.9}$$

Since the superconducting current is

$$\mathbf{j}_s = e n_s \mathbf{v}_s. \tag{A.10}$$

The last term in Eq.(A.9) equals the negative of the kinetic energy and thus exactly compensates the kinetic energy in the initial expression for the energy (A.1). Collecting all the remaining terms, we obtain the following expression for the total energy:

$$U = \int [\frac{n_s \hbar^2}{8m_s}(\nabla\varphi)^2 - \frac{n_s \hbar e}{4m_s c}\nabla\varphi \cdot \mathbf{A} - \frac{\mathbf{B}\cdot\mathbf{M}}{2}] dV. \tag{A.11}$$

Below we consider FSB. Both F and S very thin and positioned close to each other. We introduce a small distance d between the films, which in the end approaches zero. Although the thickness of each film is assumed to be small, the 2-dimensional densities of super-carriers $n_s^{(2)} = n_s d_s$ and magnetization $\mathbf{m} = \mathbf{M}d_m$ remain finite. Here d_s is the thickness of the SC film and d_m is the thickness of the FM film. The 3d super-carrier density in the SC film is $n_s(\mathbf{R}) = \delta(z)n_s^{(2)}(\mathbf{r})$ and the 3d magnetization in the FM film is $\mathbf{M}(\mathbf{R}) = \delta(z-d)\mathbf{m}(\mathbf{r})$, where $\mathbf{r}$ is the two-dimensional radius-vector and the z-direction is chosen to be perpendicular to the films. In what follows the 2d SC density $n_s^{(2)}$ is assumed to be a constant and the index (2) is omitted. The energy (A.11) for this special case takes the following form:

$$U = \int [\frac{n_s\hbar^2}{8m_s}(\nabla\varphi)^2 - \frac{n_s\hbar e}{4m_s c}\nabla\varphi\cdot\mathbf{a} - \frac{\mathbf{b}\cdot\mathbf{m}}{2}]d^2\mathbf{r}, \tag{A.12}$$

where $\mathbf{a} = \mathbf{A}(\mathbf{r}, z=0)$ and $\mathbf{b} = \mathbf{B}(\mathbf{r}, z=0)$. The vector potential satisfies the Maxwell-London equation, which is derived from the static Maxwell equation $\nabla\times\mathbf{B} = \frac{4\pi}{c}\mathbf{j}$, where $\mathbf{j}$ is the total current density on the surface of the superconductor, and is given by $\mathbf{j} = (\mathbf{j}_s + \mathbf{j}_m)\delta(z)$. The supercurrent and the magnetic current densities are given in Eqs.(A.3, A.4). Using $\mathbf{B} = \nabla\times\mathbf{A}$, the Maxwell-London equation reads

$$\nabla\times(\nabla\times\mathbf{A}) = -\frac{1}{\lambda_e}\mathbf{A}\delta(z) + \frac{2\pi\hbar n_s e}{m_s c}\nabla\varphi\delta(z) + 4\pi\nabla\times(\mathbf{m}\delta(z)). \tag{A.13}$$

The calculations become simple in the Fourier-representation. We write the Fourier transform of the vector potential $\mathbf{A}_\mathbf{k}$ as a sum $\mathbf{A}_\mathbf{k} = \mathbf{A}_{m\mathbf{k}} + \mathbf{A}_{v\mathbf{k}}$ of independent contributions from magnetization and V. Using the following definitions of the Fourier transform:

$$\mathbf{A}_\mathbf{k} = \int \mathbf{A}(\mathbf{r}, z)e^{-i\mathbf{q}\cdot\mathbf{r} - ik_z z}d^3r, \tag{A.14}$$

$$\mathbf{a_q} \;=\; \int \mathbf{a}(\mathbf{r}, z=0) e^{-i\mathbf{q}\cdot\mathbf{r}} d^2r. \tag{A.15}$$

The equation for the magnetic part of the vector-potential reads

$$\mathbf{k}(\mathbf{k}\cdot\mathbf{A}_{m\mathbf{k}}) - k^2\mathbf{A}_{m\mathbf{k}} = \frac{\mathbf{a}_{m\mathbf{q}}}{\lambda_e} - 4\pi i\mathbf{k}\times\mathbf{m}_{\mathbf{q}} e^{ik_z d}, \tag{A.16}$$

where $\mathbf{q}$ is the projection of the wave vector $\mathbf{k}$ onto the plane of the films: $\mathbf{k} = k_z\hat{z}+\mathbf{q}$. An arbitrary vector field $\mathbf{V_k}$ in wave-vector space can be fixed by its coordinates in a local frame of reference formed by the vectors $\hat{z}, \hat{q}, \hat{z}\times\hat{q}$:

$$\mathbf{V_k} = V^z_{\mathbf{k}}\hat{z} + V^{\parallel}_{\mathbf{k}}\hat{q} + V^{\perp}_{\mathbf{k}}(\hat{z}\times\hat{q}). \tag{A.17}$$

The solution to equation (A.16) with $A_z = 0$ is found by taking the inner product of equation (A.17) with $\hat{q}$, $\hat{z}$ and $\hat{z}\times\hat{q}$, respectively as below:

$$A^{\parallel}_{m\mathbf{k}} = -\frac{4\pi i m^{\perp}_{\mathbf{q}}}{k_z} e^{ik_z d} - \frac{a^{\parallel}_{m\mathbf{q}}}{k_z^2\lambda_e}, \tag{A.18}$$

$$A^{\parallel}_{m\mathbf{k}} = -\frac{4\pi i m^{\perp}_{\mathbf{q}}}{k_z} e^{ik_z d}, \tag{A.19}$$

$$A^{\perp}_{m\mathbf{k}} = -\frac{1}{\lambda_e k^2} a^{\perp}_{\mathbf{q}} + \frac{4\pi i\left(k_z m^{\parallel}_{\mathbf{q}} - q m_{\mathbf{q}z}\right)}{k^2} e^{ik_z d}. \tag{A.20}$$

Integration of the latter equation over k_z gives the perpendicular component of $\mathbf{a_q}^{(m)}$:

$$a^{\perp}_{m\mathbf{q}} = -\frac{4\pi\lambda_e q(m^{\parallel}_{\mathbf{q}} + i m_{\mathbf{q}z})}{1+2\lambda_e q} e^{-qd}. \tag{A.21}$$

It follows from Eqs.(A.18, A.19) that $a^{\parallel}_{m\mathbf{q}} = 0$. The vortex-induced vector potential is

$$\mathbf{A}_{v\mathbf{k}} = \frac{2i\phi_0(\hat{q}\times\hat{z})F(\mathbf{q})}{\mathbf{k}^2(1+2\lambda_e q)}, \tag{A.22}$$

where $F(\mathbf{q}) = \sum_j n_j e^{i\mathbf{q}\cdot\mathbf{r}_j}$ is the vortex form-factor; the index j labels the V, n_j denotes the vorticity of the jth vortex and $\mathbf{r}_j$ are coordinates of the vortex centers.

The Fourier-transform of the vortex-induced vector potential at the surface of the SC film $\mathbf{a}_{v\mathbf{q}}$ reads

$$\mathbf{a}_{v\mathbf{q}} = \frac{i\phi_0(\hat{q}\times\hat{z})F(\mathbf{q})}{q(1+2\lambda_e q)}. \tag{A.23}$$

We express the energy (A.12) in terms of the fields and vector-potential Fourier-transforms separating the purely magnetic, purely vortex and the interaction parts:

$$U = U_{vv} + U_{mm} + U_{mv}. \tag{A.24}$$

The vortex energy U_{vv} is the same as it would be in the absence of the FM film:

$$U_{vv} = \frac{n_s\hbar^2}{8m_s}\int \nabla\varphi_{-\mathbf{q}}\cdot(\nabla\varphi_{\mathbf{q}} - \frac{2\pi}{\phi_0}\mathbf{a}_{v\mathbf{q}})\frac{d^2q}{(2\pi)^2} \tag{A.25}$$

However, the magnetic energy U_{mm}:

$$U_{mm} = -\frac{1}{2}\int \mathbf{m}_{-\mathbf{q}}\cdot\mathbf{b}_{m\mathbf{q}}\frac{d^2q}{2\pi^2} \tag{A.26}$$

contains the screened magnetic field $\mathbf{b}$ and therefore differs from its value in the absence of the SC film, but it does not depend on the vortex positions. The interaction energy reads

$$\begin{aligned} U_{mv} &= -\frac{n_s\hbar e}{4m_s c}\int(\nabla\varphi)_{-\mathbf{q}}\cdot\mathbf{a}_{m\mathbf{q}}\frac{d^2q}{(2\pi)^2} \\ &- \frac{1}{2}\int \mathbf{m}_{-\mathbf{q}}\cdot\mathbf{b}_{v\mathbf{q}}\frac{d^2q}{(2\pi)^2}. \end{aligned} \tag{A.27}$$

Note that only the form-factor $F(\mathbf{q})$ conveys any information about the vortex arrangement.

VITA

Hongduo Wei was born in Liaoning, China. He received his B.S. degree from Zhejiang University in 1996. He obtained his M.S. degree from Chinese Academy of Sciences in 1999. He obtained his M.S degree from the Department of Physics at Texas A&M University in 2002. He received his Ph.D degree from the Department of Physics at Texas A&M University in 2006.

His permanent address is:
1100 Hensel Dr. Apt. Y1C
College Station, Texas 77840

The typist for this thesis was Hongduo Wei.